One Page Summary
for FNAL Proposal No. 562

A PROPOSAL TO BUILD A HIGH-INTENSITY NEUTRINO BEAM AND TO STUDY CHARM PRODUCTION

Argonne National Laboratory, Carnegie-Mellon University,
University of Kansas, Michigan State University,
Notre Dame University, and Purdue University

It is proposed to build a rapid cycling, high flux neutrino beam covering the energy range from 2 to 60 GeV. The beam is produced by 125 GeV protons incident on a production target, two horns to focus secondaries, and an iron shield to range out the muons.

Such a beam in conjunction with the 15-foot bubble chamber:

a. Will provide a copious source of charmed particles produced in simple quasi-two-body channels. A detailed study of production and decay modes will be possible.

b. Will allow a high statistics study of deep inelastic neutrino scattering, quasi-two-body reactions, and strange particle production on a reasonable time scale and at a competitive cost.

c. Should be regarded as a facility, and we indicate some other possible uses of this new beam.

We request a 10^{19} proton exposure of neutrinos with deuterium fill and 1×10^{19} protons with a light neon-hydrogen fill of the 15-foot chamber.

Fermilab Proposal No. 562

Scientific Spokesman:
L. G. Hyman
Argonne National Laboratory
Argonne, IL 60439
(312) 739-7711

A PROPOSAL TO BUILD A HIGH-INTENSITY NEUTRINO BEAM AND TO STUDY CHARM PRODUCTION

Argonne National Laboratory, Carnegie-Mellon University,
University of Kansas, Michigan State University,
Notre Dame University, and Purdue University[†]

May 20, 1977

+AUTHOR LIST

ARGONNE NATIONAL LABORATORY

M. Derrick
L. G. Hyman
P. Gregory
K. Jaeger
G. Levman
R. J. Miller
B. Musgrave
P. Schreiner
R. Singer
A. Snyder

CARNEGIE-MELLON UNIVERSITY

S. J. Barish
A. Engler
R. Kraemer
T. Kikuchi
F. Messing

UNIVERSITY OF KANSAS

R. Ammar
R. Davis
C. Eklund
N. Kwak
R. Stump
D. Zacrep

MICHIGAN STATE UNIVERSITY

R. A. Lewis
B. Y. Oh
M. Pratap
G. Sionakades
G. A. Smith
J. Whitmore

UNIVERSITY OF NOTRE DAME

J. M. Bishop
N. N. Biswas
N. M. Cason
V. P. Kenney
R. Ruchti
W. Shephard

PURDUE UNIVERSITY

V. Barnes
D. Carmony
A. Garfinkel
L. Gutay
A. Laasanen
K. Rangan

CONTENTS

I. Introduction

II. Description of the Beam.

- A. Rate Advantages of Using 125 GeV Protons
- B. Physics Analysis Advantages.
- C. The Beam as a Facility.

III. Physics

- A. Charmed Particle Production and Decay.
- B. Conventional Neutrino Physics Below 60 GeV

IV. Requested Exposure

V. The Contribution of this Collaboration.

VI. Costs

Appendices:

I. Response to Questions Raised at the ν-Workshop.

II. Possible Extensions of the Proposed Beam.

III. Recognizing Semi-Leptonic Decays of C_0^+ in Deuterium.

I. INTRODUCTION

Studies of the properties of particles having the new charm quantum number provide an important but difficult experimental challenge. Only a few states are known, and there are many important questions that must be clarified. Although most of the data to date has come from the e^+e^- storage rings, the rate of charmed particle production at Fermilab is almost certainly much higher than with the e^+e^- devices. The cross section for charm production in hadronic collisions is difficult to both estimate and measure. In addition, the large masses involved imply many decay channels and require a good trigger to enhance the signal-to-noise ratio; this has, so far, not been devised.

These considerations have led a number of groups to propose studies of the properties of charmed particles with production via the weak (ν) as well as electromagnetic (γ) interactions. While we believe both approaches are useful and should be pursued, there are aspects of the physics of charm which are best studied with a ν-beam.

In neutrino-nucleon interactions, it should be possible to measure the charm cross section with some reliability, and the complete information on each event in exclusive channels minimizes the background. Indeed, the $\mu^- e^+ K^o(\Lambda^o) + X$ events seen in the 15-foot bubble chamber probably result from the semileptonic decays of charmed mesons or baryons. Of particular interest is the structure of the charm-changing weak current[1] and the weak form factors of the charmed objects. The same information is also available from a study of semileptonic decays of those objects albeit only out to a Q^2 of $\sim 1.3\ (\mathrm{GeV}/c)^2$. Just how big the semileptonic modes are is not known for sure. If they should turn out to be very small, getting at the structure of the

charm-changing weak interaction could be done using neutrino production.

To illustrate this in the quark parton model, inclusive charm production with $\Delta C = 1$, $\Delta S = 0$ is expected to be given by

$$\frac{d^2\sigma}{dxdy} \propto 2x\, d(x) \sin^2\theta + 2x\, \bar{c}(x)\, (1-y)^2 \sin^2\theta \quad .$$

Thus a neutrino experiment in principle measures the $\sin^2\theta$ strength of the charm-changing current as well as the amount of $\bar{c}$ quark in the $q\bar{q}$ sea. If the down and the $\bar{c}$ quark have any right-handed coupling, then there will be additional contributions with a $(1-y)^2$ distribution. In the same way, it is important to extract information on quark parton distributions for $\Delta C = 0$, $\Delta S = 1$ transitions.

Some other points worth mentioning in comparing charm production by ν's and other beams are that we will probe momentum transfers in production such that $q^2_{prod.} \gtrsim 2\, Q^2_{semileptonic\ decay}$. Studies of charmed particle production using neutrino beams will then be interesting and may even be crucial for our complete understanding both of the nature of charm and of the quark-parton model.

Specific two-body neutrino interactions such as

$$\nu + p \rightarrow \mu^- + \Delta^{++} \tag{1}$$

have cross sections that rise quickly from threshold, level out, and become nearly independent of neutrino energy. This behavior results from the form factor damping of the intrinsic, linearly-rising weak cross section, and, in the case of the $\mu^-\Delta^{++}$ final state, a quantitative comparison of the theory and data has been made from the Argonne-Purdue experiment in the 12-foot chamber.[2]

Similar cross section behavior is expected for the case of charmed-baryon production in reactions such as:

$$\nu + n \rightarrow \mu^- + C_0^+ \tag{2}$$

$$\nu + p \rightarrow \mu^- + C_1^{++} \tag{3}$$

$$\nu + n \rightarrow \mu^- + C_1^+ \tag{4}$$

$$\nu + p \rightarrow \mu^- + C_1^{*++} \tag{5}$$

$$\nu + n \rightarrow \mu^- + C_1^{*+} \quad . \tag{6}$$

The masses of the above charmed baryons (~ 2-2.5 GeV) set the threshold in the 2-4 GeV neutrino energy range, as seen in Fig. 1. Since this neutrino energy is between the upper end of the Brookhaven beam and the lower end of the existing Fermilab beam, the yield of reactions (2) to (6) can be substantially enhanced by using intermediate energy protons.

We are proposing such a new high-rep.-rate ν beam which would use protons of 125 GeV, and be directed at the 15-foot chamber. With a two-horn focussing system, the peak of the ν spectrum is in the 3-5 GeV region. When the charmed baryon yields per unit time are compared for the existing 400 GeV beam and the proposed beam, the latter has nine times the rate.

Our initial interest is in studying the production and decay properties of charmed particles. We consider that an exposure of 10^{19} protons with a deuterium fill and a similar exposure of 10^{19} protons with a light neon-hydrogen fill are required. We anticipate, given the participation of the six groups in the proposal, important results on charm will appear about nine months after the exposures are taken.

In order to accomplish the project, we are prepared to design and build the horns and their power supplies, to help with the design of the beam and to devise the flux normalization procedures needed to exploit the high statistics data provided by such a facility. We urge that completion of the facility

be aimed for no later than two years from the time of writing this proposal. This beam should be regarded as a facility, and we discuss this in Section II. C.

In this proposal, we outline the features of the beam, and then discuss the charm physics as well as the conventional physics we propose to study. In the appendices, we discuss

I. The questions asked by the ν Workshop Review Committee.

II. The possible extension of the facility to a high flux ν_e, $\bar{\nu}_e$ beam and to a dichromatic beam.

III. Recognizing semileptonic decays of charmed baryons.

II. DESCRIPTION OF THE BEAM

A. Rate Advantages of Using 125 GeV Protons

The ν beam we consider uses a primary proton energy of 125 GeV. The protons strike a production target, followed by a two-horn system to focus the secondaries. There is a decay space of 175 meters which ends at a steel shield 75 meters long. Such a facility can be installed utilizing the N-5 beam which presently delivers hadrons to the 15-foot chamber. This beam can be used to transport full intensity 125 GeV protons provided the shielding is improved. In Fig. 2, we show an overlay on a standard Fermilab print of some of the changes that would have to be made.

The immediate question is how much improvement does this beam provide over the standard 400 GeV beam. To answer this question, one must decide how to calculate the flux from the two beams. Different parameterizations of the π^+, K^+ yields differ significantly, so that the absolute yields are consequently difficult to calculate. We have chosen the Wang[3] parameterization for π^+ and taken a 10% K^+/π^+ ratio at both energies. The Wang formula has been fit to a large variety of pp data, and it also fits the thick target Fermilab 200 GeV data.[4] The quality of the fit of the Wang formula, to some representative pp data at 102 GeV/c,[5] is shown in Fig. 3. With the Wang formula and the computer program NUADA,[6] we compute the flux shown in Fig. 4.

The number of events in deuterium for reactions (2) through (6), as well as the inclusive charged current event numbers, are shown in Table I. We note from Table I that the proposed beam produces nearly four times as many charmed baryons per primary proton in the exclusive channels listed as does the 400 GeV beam. The 125 GeV total charged-current neutrino interaction rate is about 1.7 times larger than the 400 GeV

rate per proton. For completeness, Fig. 5 shows the $\bar{\nu}$ flux obtained with the proposed beam.

In addition to the higher event rates/picture, the 125 GeV beam also has a substantial repetition rate advantage. The cycles for dedicated running are shown in Fig. 6. The low energy beam can be run 2.5 times as fast. Thus, in dedicated running, the proposed beam produces the exclusive charm channels at about 10 times the rate at 400 GeV. Furthermore, since radiation damage and target melting, etc. presumably scale with the electromagnetic cascade, the 125 GeV beam can use the full extracted intensity, whereas the present beam, at least at this time, is limited to 1.0×10^{13} ppp. So the overall rate (per unit time) could be as much as 25 times higher.

Finally, this is an excellent beam to use when the Laboratory wants to cut its power bill. The ohmic loss per pulse in the main ring is down by a factor of approximately 40 for the 125 GeV beam. Thus, in the dedicated running mode, the 125 GeV will have a main ring power bill which is down by a factor of 15 from dedicated 400 GeV running.

This is perhaps a good time to point out that the 125 GeV beam really adds a new dimension to the Laboratory's neutrino program. With the 400 GeV beam, present experiments have difficulty obtaining more than a few 10^{18} protons on target. With the 125 GeV beam, exposures of 10^{19} can be attained. In fact, with an overall efficiency of 0.50 and an intensity of 2.5×10^{13} ppp, a 10^{19} proton run would take less than one month.

In comparing the data rates possible with 125 and 400 GeV protons:

a) For the same ppp and repetition rate, the data rate with 125 GeV protons is higher for $E_\nu \leq 20$ GeV.

b. Taking advantage of the increased repetition rate possible at 125 GeV, the data rate is higher for $E_\nu \leq 36$ GeV.

c. Since extracted proton intensities up to 2.5×10^{13} are possible with 125 GeV protons, this extends the crossover $E_\nu \sim 50$ GeV.

B. Physics Analysis Advantages

The intermediate energy beam has the advantage that we are operating close to threshold, and more complex states with several missing neutrals will be suppressed relative to the simple two-body final states we are seeking to isolate. This is important in any D_2 running as we will want to separate the two-body production reactions from the background by use of kinematic fitting. The ability to reject unseen π^0's in D_2 depends on the transverse momentum imbalance which is detectable. In the high energy beam, the most probable neutrino energy making a C_0^+ is $E_\nu = 17$ GeV. While in the intermediate energy beam, it is 5 GeV. In the proposed beam, the μ^- will have a momentum of $\approx$ 4 GeV and $\delta p/p \approx 0.008$ or $\delta p = 32$ MeV/c, while in the high energy beam, the outgoing muon will have momentum $\approx$ 14.5 GeV and $\delta p/p \approx 0.02$ or $\delta p = 290$ MeV/c. So we would expect events with missing neutrals to be suppressed because we are closer to threshold, and if they do occur, they are more likely to signal their presence with momentum imbalance.

C. The Beam as a Facility

We regard this beam as a facility. We envisage there will be additional proposals for the 15-foot chamber, as well as for counter type experiments. For example, tagged-emulsion experiments searching for short-lived objects would benefit from this beam. Such experiments could easily progress to leaving out the emulsion and isolating the charm states by purely electronic means. There may be some advantages for this beam to do $\nu_\mu + e^- \rightarrow \nu_\mu + e^-$ or $\bar{\nu}_\mu + e^- \rightarrow \bar{\nu}_\mu + e^-$. In Appendix II we mention a possible modification of the beam to provide a higher energy ν_e beam.

An important consideration is the likelihood of dedicated running. It is clear that one of the big advantages of the beam is the rapid cycle rate. The 125 GeV beam is 2.4 times faster than dedicated 400 GeV running and 4 times faster than the usual 10 second 400 GeV running. A significant point is that the power bill is a major cost at the laboratory. The fact that this 125 GeV mode of operation uses less than 1/15 of 400 GeV main ring power is important and may allow the laboratory to schedule more research time. Such considerations may be particularly relevant for doubler operation, when, during the long ramp and flat-top, the 125 GeV dedicated operation could easily be run in parallel with the 1000 GeV counter program.

III. PHYSICS

A. Charm

The direct observation of charmed-baryon production in two body reactions by neutrinos is topical physics. Several calculations[7, 8, 9] of the reactions (2-6) have been made and they are all in rough accord. We have used the work of Avilez et al. shown in Fig. 1. All of the calculations use the GIM mechanism and the charm changing current ($\approx \sin^2\theta_c$) to change an ordinary down quark into a charm quark. The calculations rely on SU(4) to obtain the $q^2_{prod.} = 0$ normalizations. SU(4) breaking effects are incorporated at the quark level by introducing quark mass breaking. To obtain the $q^2_{prod.}$ behavior, dipole form factors are used with charmed mesons setting the mass scale. The resultant cross sections are quite large; for example, the asymptotic cross section for $\mu^- C_0^+$ is approximately 60 % of $\mu^- \Delta^{++}$.

The first obvious and important set of experiments is to establish the magnitude of the cross sections, the q^2 dependence, the energy behavior, the mass and width of C_1^{*++}. Here one expects the C_1^{*++} to decay strongly i.e. $C_1^{*++} \rightarrow \pi^+ + C_0^+$. Similarly for the C_1^{++}, if its mass exceeds the C_0^+ by more than a pion mass. On the weak non-leptonic decays of the C_0^+, the experiment will give information on branching ratios, including the search for the presence of intermediate resonances in the decay products such as $C_0^+ \rightarrow Y_1^{*+} \pi^+ \pi^-$.
$\hookrightarrow \Lambda^o \pi^+$

As is well known, the large available energy will lead to many decay

modes. In an analysis by B. Lee et al.,[10] they expect the channels

$$C_0^+ \rightarrow \Lambda^o \pi^+ + m\pi \tag{7}$$

$$C_0^+ \rightarrow \Sigma\pi + m\pi \tag{8}$$

$$C_0^+ \rightarrow \bar{K}N + m\pi \tag{9}$$

to be important and

m = 0	occurs for ~20% of the decays
m = 1	30%
m = 2	25%
m = 3	15%
m = 4	5%

Those modes which do not have neutral pions should be relatively easy to isolate. This is because of the narrowness of the C_0^+. Putting in reasonable values for the track errors in decays such as

$$C_0^+ \rightarrow \Lambda^o + \pi^+ \tag{10}$$

$$C_0^+ \rightarrow \Lambda^o + \pi^+ + \pi^+ + \pi^-, \tag{11}$$

we obtain a mass resolution which has a FWHM of 45 MeV. Calculations on the nature of the background from associated production. e.g. $\nu + n \rightarrow \mu^- + \Lambda^o + K^+ + X$ indicate the Λ + mesons effective mass obtained is widely dispersed over the mass scale and will not provide much background. The results of Deden et al. in Gargamelle[14] indicate there are 22 examples of $\nu + N \rightarrow \Lambda^o + K^+ + X$

events and (42 ± 20) unassociated Λ^o's. Assuming the topological distributions for $\Lambda^o + K^+ + X$ and for $C_0^+ \to \Lambda\pi^+ + X$ to be approximately the same, we can then normalize the background contribution from associated production, as shown in Fig. 7.

From isospin bounds[11] one can place limits on the fraction of a given channel which will have no missing neutrals, for example, $\Lambda^o\pi^+\pi^+\pi^-$ is between 1/2 and 4/5 of all $\Lambda^o\pi^+(\pi\pi)$. Similar considerations hold for the $\Sigma\pi$ channels, so that an appreciable fraction of the decays can be isolated even without π^o detection.

As an example, we estimate how many $C_0^+ \to \Lambda^o\pi^+$ we expect to identify. The result is obtained by applying the following factors to the number, 4,000 C_0^+ produced (Table I); $\frac{1}{3}$ (decaying via reaction (7)), $\frac{1}{5}$ (with m = 0), $\frac{2}{3}$ (Λ visibility), 0.9 (hadronic decay). This gives 160 events.

The program described above should be carried out in a D_2 bubble chamber; a well-understood and well-monitored beam is an important part of the experiment. The number of $\nu p \to \mu^- \Delta^{++}$ events is ≈ 13,000, so that a direct flux independent cross section comparison above charm threshold is possible.

Perhaps the most interesting physics will come from a study of the C_0^+ semileptonic decays $C_0^+ \to \Lambda^o \{\mu^+_{e^+}\} \nu$. As pointed out by several authors,[9, 12] this is an excellent reaction to test the structure of the charmed currents. In the GIM scheme, $J^\lambda = \bar{s}\gamma^\lambda (1 - \gamma_5) c \cos\theta$. This is generalized to (keeping vector and axial vector couplings only) $J^\lambda = \bar{s}\gamma^\lambda (g_V - g_A\gamma_5) c \cos\theta_c$. Buras and

Ellis[12] have worked out various decay distributions as well as the Λ polarization. Fig. 8, taken from Ref. 12, illustrates the difficulties involved in trying to extract information on the couplings by measuring quantities such as the mass spectrum of the Λe system (Fig. 8a), the average Λe mass (Fig. 8b), or the average lepton energy (Fig. 8c). In all of these examples, there is not much discrimination between the various couplings.

A much more sensitive probe comes from the Λ^o polarization which gives rise to an up-down asymmetry for the $\Lambda^o \to p\pi^-$. In the Λ^o rest frame, it will be polarized along the directions $\hat{\alpha}$ and $\hat{\beta}$, which are unit vectors made up from the sum and difference of unit momentum vectors along the decay leptons. Fig. 9(a) shows the polarization along $\hat{\alpha}$ and $\hat{\beta}$ for different choices of the couplings. Fig. 9(b) illustrates the projected distribution. Fig. 10 shows a Monte Carlo run of 100 experiments, each with 100 events. Each experiment was analyzed using a likelihood function of the form

$$\frac{dP}{d\cos\psi_{\binom{\alpha}{\beta}}} = \frac{1}{2}\left[1 + G_{\binom{\alpha}{\beta}} \cos\psi_{\binom{\alpha}{\beta}}\right] \tag{12}$$

for the two projected distributions along $\hat{\alpha}$ and $\hat{\beta}$. The sample was generated with the phase and magnitude expected for V-A. It is clear from Fig. 10 that the analysis strongly favors V-A over V, A, V + A.

The authors of Ref. 9 have gone further and show that the C_0^+ is expected to be strongly polarized in the production process, and the polarization

lies in the production plane. The polarization of the C_0^+ rotates in the plane as a function of $q^2_{prod.}$, but its magnitude is large and roughly independent of $q^2_{prod.}$ They show that there is a Λ^o asymmetry about the C_0^+ polarization direction. The degree of this asymmetry depends on the magnitude of C_0^+ polarization as a function of $q^2_{prod.}$ (this dependence is weak), and the Q^2_{decay}, the momentum transfer in the decay. This asymmetry is a measure of the relative amounts of vector and axial vector currents, but it does not distinguish their sign. i.e. can't tell V-A from V+A.

In a subsequent preprint,[13] the authors of Ref. 9 calculate the Λ^o polarization given that the parent C_0^+ is polarized. The authors show that if the decay lepton variables are averaged over and the Λ^o direction is averaged over, then the mean longitudinal polarization of the Λ is independent of the production variables and identical to the case of unpolarized decay. As seen earlier in Fig. 10, this longitudinal polarization is sensitive to the relative sign of (V±A) and readily distinguishes between the two cases.

It is also shown that the Λ^o polarization relative to the production plane is proportional to the C_0^+ polarization, and the coefficient is a strong function of Q^2_{decay}. This then can be used to determine the C_0^+ polarization and probe the V, A structure of the production process.

One will certainly try to detect terms which vanish with time-reversal invariance, e.g. C_0^+ polarization normal to the lepton plane. Another test is to search for a correlation between the normal to the C_0^+ decay plane and

the C_0^+ polarization.

The semileptonic branching ratio $C_0^+ \rightarrow \Lambda^0 \{^{\mu}_{e}\} \nu$ is not yet well measured,[14] but if it is about 10%, we expect 270 events in D_2. We require e and μ identification to identify these events. This is discussed in Appendix III. It would be preferable to use a hydrogen-neon mixture for this aspect of the experiment. The rate is about 3x higher and μ-e identification is straightforward. In light neon, the event rate (charged + neutral) is $\approx$ 0.3 events/frame at 10^{13} ppp, so this may be close to the practical limit on the intensity.

B. Conventional Neutrino Physics Below 60 GeV

The study of charged and neutral current $\nu_\mu, \bar{\nu}_\mu$ interactions at the lower energy accelerators has given a first look at νN interactions in the energy range $E_\nu \leqslant 12$ GeV.[15,16] At the ZGS, the deuterium filled 12-foot bubble chamber will complete its program of νn and νp interactions at low energies. At the CERN proton synchrotron, the heavy liquid chamber Gargamelle has been used in an extensive study of ν and $\bar{\nu}$ interactions on complex nuclei. The inclusive νN and $\bar{\nu} N$ differential cross section can be written as

$$\frac{d^2\sigma^{\nu,\bar{\nu}}}{dxdy} = \frac{G^2ME}{\pi}\left[(1 - y - \frac{Mxy}{2E})\, F_2(x) + \frac{y^2}{2}\, 2\, x\, F_1(x) \pm (y - \frac{y^2}{2})\, x\, F_3(x)\right] \quad (13)$$

where $x = Q^2/2M\nu$ and $y = \nu/E$. The Gargamelle experiment has determined F_1, F_2 and F_3 for a neutron-proton average in the scaling region $W^2 > 4$ GeV^2 and $Q^2 > 1$ GeV^2. The analysis was based on a sample of 635 ν and 156 $\bar{\nu}$

events with $2.5 < E_\nu < 12$ GeV. The only continuing program at the lower energy machines will be that using the 7 ft. chamber at Brookhaven. However, as discussed later, for the standard exposure of 10^{19} protons, the proposed beam with the 15 ft. chamber provides more than 12 times as many charged current events than does the 7 ft. chamber. The experiments now being carried out using 400 GeV protons at FNAL and the CERN SPS will study the region $E_\nu > 10$ GeV.

In this experiment we propose to study neutrino nucleon interactions with a high precision: one that compares to that of eN interactions studied at SLAC and Cornell. The proposed experiment allows a detailed study of both inclusive and exclusive channels in charged current reactions and of inclusive neutral current processes, up to $E_\nu \sim 60$ GeV. A complete program encompasses both ν and $\bar{\nu}$ beams with H_2, D_2 and neon-hydrogen fillings of the bubble chamber. A combination of the bubble chamber technique and a high flux beam with well-known normalization provides a powerful technique for implementing such a program. In this section of the proposal, we briefly outline some of the areas of physics that require a high statistics experiment. For purposes of discussion, we concentrate mainly on ν-D_2 and $\bar{\nu}$ - D_2 interactions.

1. Structure Functions and Scaling

An important question is the energy dependence of the total cross section off protons and neutrons separately for ν and $\bar{\nu}$ beams in the energy range 2-60 GeV. Relying on the experience of the CERN group working

at the PS and SPS, an accuracy of ±10% in flux normalization can be realized.[17]

The inclusive charged current rates for a ν D_2 exposure are shown in Table II. Also shown for comparison are the charged current rates for the same size exposure at Brookhaven. The separation of events into neutron and proton interactions is not difficult and has been done in our ZGS experiment.[16] The structure function analysis is of particular interest in the scaling region $W^2 > 4$ GeV^2, $Q^2 > 1$ GeV^2; these selections substantially remove all of the low multiplicity channels which are dominated by such quasi-two body processes as those listed in Table III. However, we will have two orders of magnitude more events than any experiment to date. Fig. 11 shows the expected hadronic mass (W) distributions in νp collisions for all Q^2 and for $Q^2 > 1$ GeV^2. For $Q^2 > 1$ GeV^2, there will be 43,600 charged current νp events, see Fig. 12. For $Q^2 > 1$ GeV^2 and $W^2 > 4$ GeV^2, there will be 38,500 νp charged current events.

As is obvious from Eq. (13), one can determine the structure functions F_1, F_2, F_3 using suitable combinations of ν and $\bar{\nu}$ differential cross sections. However, given high statistics data extending over a substantial energy range it is possible to determine F_1, F_2, and F_3 for neutron and proton targets from ν - D_2 alone.

A precise measurement of $F_2(x)$ and $xF_3(x)$ will allow, for the first time an incisive test of the Adler[18] and and Gross-Llewellyn Smith[19] sum

rules in neutrino interactions. Note that these determinations are for the neutron and proton targets separately and are free from complications of secondary interactions in a nucleus.

The inclusive charged current data will also allow a search for charge symmetry violations. While the Gargamelle results are consistent with charge symmetry[15], results from the HPWF experiment suggest this symmetry is violated for $E_\nu \geqslant 30$ GeV.[20] This test is done by comparing normalized ν and $\bar{\nu}$ cross sections at $x = 0$.

As pointed out by Holstein and Treiman,[21] the introduction of second class currents would alter these sum rules for the inelastic-neutrino structure functions. While this is not expected to afford the most incisive probe for second class currents, a detailed test of these sum rules is long overdue.

Adler has shown,[22] in the approximation where the outgoing lepton mass is ignored, that the amplitude for forward, inelastic lepton scattering (outgoing μ parallel to the neutrino) is proportional to the matrix element of the divergence of the weak current. In the absence of second class currents and provided the first class currents obey CVC, only axial vector currents contribute in the forward limit i. e. no parity violating effects occur in this limit. Discovery of parity violating correlations for forward inelastic lepton scattering would either rule out CVC for first class currents or imply the existence of second class currents. The experimental evidence on these issues is too limited to draw any conclusions.[23] The results are consistent with PCAC

within a factor of two. Such a study can only be pursued if high statistics normalized data are available to select a sufficiently small lepton angle.

Measurements of the quark distribution functions, u(x) and d(x), are of central importance in the quark-parton model. By using deuterium as a target, and γ converting plates in order to improve the hadronic energy resolution, it is possible in one experiment to measure the absolute value (not just the shape) of the ratio of the down to up quark distributions as a function of x. For example, when $x \geqslant 0.2$ (where the sea contributions are small) one has

$$R = \frac{d(x)}{u(x)} = \frac{d\sigma}{dx}_{\nu p} \Big/ \frac{d\sigma}{dx}_{\nu n} \tag{15}$$

Many theorists regard the large x behavior of this ratio to be of high importance, but are not able to make unique predictions. For example, R. Feynman predicts $R \to (1 - x) \to 0.0$ as $x \to 1.0$, while G. Farrar predicts that $R \to 0.20$[24]. We will be able to make precise measurements of R for $x \leqslant 0.7$.

2. Quasi Two and Three Body Processes

A principal interest in such reactions has been the determination of axial vector form factors. The simplest and, in fact, the only processes studied so far are:

$$\nu n \to \mu^- p \tag{16}$$

$$\nu p \to \mu^- \Delta^{++} \tag{17}$$

$$\hookrightarrow \pi^+ p$$

$$\nu n \rightarrow \mu^- \Delta^+ \tag{18}$$

$$\bar{\nu} p \rightarrow \mu^+ n \tag{19}$$

The only data using a D_2 target are from the Argonne experiment.[25] $\Delta^{++}(1236)$ production is complex, and one needs high statistics data. In the proposed experiment, we will be able to study the structure of the axial current with the precision that one now has for the vector current.[26] With the proposed experiment, one can also look for higher mass N^*'s, e.g.

$$\nu n \rightarrow \mu^- N^{*+} \tag{20}$$

$$\hookrightarrow p\pi^+\pi^-$$

$$\hookrightarrow \Lambda K^+$$

The expected rates for some resonance production processes are shown in Table IV, calculated using a model by P. Zucker.[27] The expected populations of some of the simpler exclusive channels relevant to these studies are shown in Table III.

While the most definitive search for the existence of second class currents possible with neutrino reactions is a study of

$$\nu p \rightarrow \mu^- \pi^+ p \tag{21}$$

$$\bar{\nu} n \rightarrow \mu^+ \pi^- n \tag{22}$$

tests can be made using the q^2 dependence of reaction (16) and the energy

dependence of the cross section for reaction (17).

Table V gives the cross section for reaction (17) at beam energies of 2 and 6 GeV when the second class current coupling constant g_{II} is set to 0, and $-6F_A(0)$, a value suggested by some nuclear physics results.[28] Such large second class current effects will be easily measurable since we will know the flux to an accuracy of 10%. Note that since second class current contributions to the total cross section for quasi-elastic scattering are small, the ratio of cross sections for reactions (17) and (16) provides a flux independent normalization.

We write the hadronic matrix element for quasi elastic $\nu_\mu - n \rightarrow \mu^- p$ scattering as

$$\Gamma_\lambda = \gamma_\lambda F_{V1} + i\sigma_{\lambda\nu} q^\nu \xi F_{V2} + \gamma_\lambda \gamma_5 F_A + \frac{\gamma_5 (P_n + P_p)_\lambda F_{A3}}{M} \qquad (23)$$

using the notation of Llewlyn Smith.[29] In Fig. 13 we show the differential cross section for various assumptions on the magnitude of the second class current contribution as measured by the normalization constant for the form factor F_{A3}. In each case a sample of 10,000 events is generated for $q^2 > 0.05$. We assume dipole form factors, CVC to fix the vector mass, $M_A = 950$ MeV, $F_A(0) = -1.23$, and $M_{A3} = 1000$ MeV. We also assume $F_{V3} = F_p = 0$. The second class current strength indicated by some nuclear physics experiments is clearly within the scope of detection of this experiment just by measuring the shape of the q^2 - distribution.

The question of which channels form the bulk of the total cross section for $E_\nu \geqslant 5$ GeV is an open one. A recent re-evaluation of the production cross sections ρ, A_1 ω^o etc. based on vector dominance and electro-production results[30] gives the yields in Table VI for reactions;

$$\nu p \rightarrow \mu^- p \rho^+ \tag{24}$$

$$\nu p \rightarrow \mu^- p A_1^+ \tag{25}$$

$$\hookrightarrow \pi^+ \pi^+ \pi^-$$

There is some disagreement on how the form factors should be included in these calculations. For comparison we also show in Table VI the event rates obtained by Gaillard et al.[31] One notes the large difference between these predictions. Other reactions can also be studied e. g.

$$\nu p \rightarrow \mu^- \Delta^{++} \rho^o \tag{26}$$

$$\rightarrow \mu^- \Delta^{++} \omega^o$$

$$\hookrightarrow \pi^+ \pi^- \pi^o \tag{27}$$

The production cross sections are small and a high statistics experiment is essential to measure them. Systematic studies of this kind for deep inelastic neutrino, electro and muo-production are particularly interesting for the diffractive events as the properties of the W meson exchange show directly. For neutral current reactions whose form is still not known they will be of even greater interest.

3. Strange Particle Production

Strange particle production by neutrinos has been observed through

$\Delta S = 0$ associated production and through $\Delta S = 1$ processes.[32]

In the case of associated production, many of the channels are well constrained although little information exists on them

$$\left.\begin{array}{l} \nu n \to \mu^- K^+ \Lambda^o \\ \nu n \to \mu^- K^o \Sigma^+ \\ \nu n \to \mu^- p K^o \bar{K}^o \\ \nu n \to \mu^- p K^+ K^- \\ \nu p \to \mu^- K^+ \Sigma^+ \\ \nu p \to \mu^- K^+ \Sigma^{*+} \\ \qquad\qquad \hookrightarrow \Lambda^o \pi^+ \end{array}\right\} \tag{28}$$

The production of positive strangeness mesons by neutrinos is allowed in the quark-parton model via sea quark transitions leaving K^+ or K^o

$$\begin{array}{l} \nu + \bar{u} \to \bar{s} + \mu^- \\ \nu + s \to u + \mu^- \end{array} \tag{29}$$

An estimate of the rate for such $\Delta S = \Delta Q$ transitions assuming an SU(3) symmetric $\bar{q}q$ sea is

$$\sigma_T (1 - B) \tan^2 \theta_c \tag{30}$$

where

$$B = \frac{q - 2\bar{q}}{q} \tag{31}$$

With $\tan^2\theta_c = 0.05$ and $\langle B \rangle = 0.80 \pm 0.06$ the rate is[32] 0.01 ± 0.003. Thus we expect to have $\approx 300 - 500$ observable examples of $\Delta S = \Delta Q$ events. This will allow a detailed probe of the x dependence of the sea using reactions like

$$\begin{aligned} \nu p &\to \mu^- p \pi^+ K_s^o \\ &\to \mu^- p K^+ \\ \nu n &\to \mu^- K_s^o p \end{aligned} \tag{32}$$

Some of the $\Delta S = \Delta Q$ allowed reactions for anti-neutrino nucleon scattering are:

$$\bar{\nu} p \to \Sigma^o \mu^+ \tag{33}$$

$$\bar{\nu} p \to \Lambda^o \mu^+ \tag{34}$$

$$\bar{\nu} n \to \Sigma^{*-}(1385)\, \mu^+ \tag{35}$$

$$\hookrightarrow \Lambda \pi^-$$

We expect 390 observable events in the case of reaction (34). The Λ^o polarization can be studied, which checks time-reversal invariance and is related to the question of second class currents.

4. Neutral Current Studies

The need for studying both ν and $\bar{\nu}$ neutral current processes off neutron and proton targets has been stressed in previous proposals.[33] We emphasize that the proposed facility complements the previous proposals by allowing a comprehensive study, for $E_\nu < 30$ GeV, of the following topics:

(a) Measurement of $R_{\nu n}$, $R_{\nu p}$, $R_{\bar{\nu} n}$, $R_{\bar{\nu} p}$, the ratios of neutral current to charged current rates.

(b) Space-time structure of the neutral current using the model dependent analysis suggested by Hung and Sakurai[34] and the model independent analysis suggested by Wolfenstein and Wyler.[35] While some parts of this program can be accomplished using iso-spin zero targets, a complete study involves proton and neutron targets and ν, $\bar{\nu}$ beams.

(c) I-spin information from exclusive channels such as $\nu n \rightarrow \nu n \pi^+ \pi^-$ and $\nu p \rightarrow \nu p \pi^+ \pi^-$ where any difference between these cross sections implies a non-zero isoscalar-iso-vector interference term. The detailed study of exclusive neutral current channels requires a narrow band beam which may well be possible in the short beam line proposed. This opens the possibility of looking for parity violating effects in reactions like $\nu p \rightarrow \nu p \pi^+ \pi^-$.

(d) Strange particle production, which is essentially un-probed, and statistics allowing a check for parity conservation in reactions like $\nu n \rightarrow \nu \Lambda^o K^o$, $\nu K^+ \Lambda^o$.

IV. REQUESTED EXPOSURE

Our basic goal is to study the production and decay properties of charmed baryons. We consider this best achieved with a ν exposure of 10^{19} protons in D_2 and with a similar exposure of 10^{19} protons in a light hydrogen-neon mixture. While it is our present belief that we would split the exposure in this manner, we hope that the final decision can be made at a time nearer to the actual running of the experiment. It is worth pointing out that in addition to running in a dedicated mode, this beam could also run simultaneously with the 400 GeV beam or with the doubler.

In addition to the ν exposure, an $\bar{\nu}$ exposure of 10^{19} protons with D_2 fill is clearly desirable. Such an exposure will allow the needed detailed study of νN and $\bar{\nu} N$ physics. If this beam is built, we would expect other groups to participate in the program opened up by studying such complementary exposures.

V. THE CONTRIBUTION OF THIS COLLABORATION

We propose to construct the two horns, power supplies, and auxiliary equipment at Argonne. We have built such devices for the current ZGS ν-facility and anticipate that the new horns could be completed within 12 months of approval. As we have mentioned, we believe that good knowledge of the ν flux is important in this experiment. There are several ways to attack this, and we would try to tie several of them together. Some obvious techniques are:

i) $\mu^-\Delta^{++}$ cross section is flat beyond 2 GeV. We expect 13,000 $\mu^-\Delta^{++}$ events, so the flux accuracy in the region of peak is about 5%. Since as part of our proposal we want to search for second class currents and they can cause the asymptotic region to shift to higher energies, we need some independent checks.

ii) Measurement of π^+ and K^+ yields from thick targets at enough momenta and angles so that the ν flux can be calculated. This needs good proton intensity monitoring and, as implemented at Argonne, has given a precision in the 10-15% region.

iii) Measurement of muon yields at different locations in the shield. This method uses ionization chambers and has been carried out by the CERN group[17] in both the PS ν beam and the SPS narrow-band beam. This is a large undertaking, but has produced a precision at the 10% level.

iv) The linear rising cross section can be used to obtain a statistical accuracy of better than 5% in 1 GeV bins for energies as high as 50 GeV. We would anticipate achieving $\approx$ 10% accuracy over the interesting dynamic range. It is our present feeling that methods ii) and iv) will provide a normalization independent of second class current effects in i) and then all three can be used to normalize charm cross sections.

The ν beam will require good monitoring and control. Many members of this collaboration have had extensive experience with this kind of ν beam, and we are in a position to develop and build the appropriate hardware, install it, and make it operational.

VI. COSTS

	Cost $	With Existing Facilities $
Horn, Power Supplies, Cables;	270 K	200 K
Improvement to Enclosures 103, 105, 106, 107, 109, 111	280 K	280 K
Steel Shield	1300 K	250 K
Drift Tube	215 K	215 K
Horn Enclosure	65 K	65 K
Utilities Modification	50 K	50 K
	Total:	1060 K

The existing power supplies for the horns at the ZGS can likely be used to save the $70K shown above. To save the $1050K on steel, we would have to request and obtain the 7000 tons of steel from the ZGS. There is presently ≈ 10,000 tons in the Argonne ν beam, but the ZGS Booster IPNS project also will require steel, and the details will have to be worked out.

We thank W. Praeg at ANL for the cost estimates on the horn. The precision is ≈ ±15%. We are indebted to Wayne Nestander of FNAL who costed the other items. The precision of the estimate is ≈ ±30%.

APPENDIX I

Response to Questions Raised at the Neutrino Workshop

At the workshop, the panel raised several questions which, paraphrased, are:

(A) What do the ν runs in light neon E-28 (Fry)[36] and heavy neon E-53A (Baltay)[37] say about charm production?

(B) What would be the effects of the iron shield being close to the bubble chamber?

(C) What is likely competition from e^+e^- storage rings at SPEAR and Cornell?

(D) What is the expected competition from the proposed-tagged photon beam spectrometer at FNAL?

Regarding question (A), we will use the calculations in this proposal to predict what should be seen in the two neon experiments and then compare to what is actually observed. For the semileptonic decay $C_0^+ \to \Lambda^o e^+ \nu$, we write

$$N = A_c N_c \frac{\Gamma_{semi}}{\Gamma_{total}} R \epsilon_{e^+} \frac{\Gamma(\Lambda^o \to p\pi^-)}{\Gamma_{total}} \epsilon_\Lambda ,$$

where

(i) A_c is the ratio of exclusive C_0^+ to charged currents in the 400 GeV beam, taken as 0.008.

(ii) N_c is the total number of charged-current events in the experiment.

(iii) Γ_{semi}/Γ is the fraction of C_0^+, which decay $C_0^+ \to \Lambda^o e^+ \nu$, taken as 0.1, and R is the ratio of e^+ to all ℓ^+, taken as 0.5.

(iv) ϵ_{e^+} is the efficiency for scanning and identifying electrons, taken as 0.8.

(v) $\Gamma(\Lambda^o \to p\pi^-)/\Gamma_{total}$ is the ratio of visible Λ decays to all Λ's, taken as 2/3.

(vi) ϵ_Λ incorporates the loss for close-in Λ's as well as that due to scanning efficiency, taken as 0.7.

(vii) N is the estimated size of event sample.

Similarly, in the hadronic mode, we have

$$N = A_c N_c \frac{\Gamma_{hadron}}{\Gamma_{total}} UVW \frac{\Gamma(\Lambda^o \to p\pi^-)}{\Gamma_{total}} \epsilon_\Lambda ,$$

where now

(i) $\Gamma_{hadron}/\Gamma_{total}$ is the branching ratio to hadrons, taken as 0.9 of hadronic decays.

(ii) U is the fraction of hadronic decays going to Λ^o in the final state, taken as 2/3.

(iii) V is the fraction of events without missing neutrals, taken as 0.5.

(iv) W is the appropriate factor for speaking of a particular state such as $\Gamma = \Lambda + m\pi$ /all Λ; m = 3.

All the other factors are defined above.

E-28 has 4200 charged-current events and E-53 has 25,000. The table below shows the expected rates together with what has been observed.

Process	E-28		E-53	
	Expected	Observed	Expected	Observed
$\nu + n \to \mu^- + C_0^+$, $C_0^+ \to \Lambda^o e^+ \nu$	0.63	None	4.3	1 Cand.
$\nu + n \to \mu^- + C_0^+$, $C_0^+ \to \Lambda^o$ + charged pions	4.7	No Evidence of structure	28	No peaks with more than 50 events

Note that for the decay into hadrons, we have lumped together all the Λ+ charged pion channels. The disagreement between the expected semileptonic rate for E-53 and the observed rate indicates something is not correct. It would imply that there is something wrong in the product $\sigma(C_0^+)\,\Gamma_{semi}/\Gamma_{total}$ we have used. We have taken $\Gamma_{semi}/\Gamma_{total} = 0.10$ and this is a guess. The true value could be smaller. In fact, perhaps the semileptonic decays are not dominantly $\Lambda\{{}^{e}_{\mu}\}\nu$ events, but perhaps states such as $\Lambda(1405)$, $\Lambda(1670)$, etc. dominate. Some recent calculations[38] indicate these states while perhaps contributing are not expected to dominate.

A prudent (90% confidence) upper limit on $\sigma\ \Gamma_{semi}/\Gamma_{total}$ from E-53 is 90% of the value that we have used throughout this proposal. There is an additional factor which causes some confusion. Our flux calculation for 400 GeV gives an inclusive charged-current counting rate for E-53, which is a factor of 1.5 times higher than they observe. So assuming this same factor prevails at 125, we can scale the E-53 semileptonic rate to our proposed neon experiment:

$$N(E=125) = N\alpha\beta = \frac{N(\text{Exp. } 53)\ Cr\alpha\beta}{1.5}$$

where

(i) r is the ratio of protons on target in the two experiments, taken as 20.

(ii) C is the charm baryon production ratio per proton, taken as 4.

(iii) α comes from using both e^+ and μ^+ and keeping losses of e^+ and Λ's smaller than in Baltay's present experiment, taken as 2.7.

(iv) β is the ratio of liquid density in the two experiments, taken as 1/2.

So with 1 event observed in E-53, N(E=125) = 108; with 3.9 events, the upper bound in E-53, N(E=125) = 421. Neither E-28 or E-53 appears to limit the hadronic modes. If we knew that $\Gamma \to \Lambda e^+\nu\ /\Gamma \to \text{all} > 0.05$, then we would have to conclude (assuming preliminary E-28, E-53 results are correct) that

the theoretical cross sections are overestimates and the number of events in the hadronic modes should be reduced accordingly.

B. One concern is the effect of the steel on the magnetic field of the 15-foot chamber and the resultant forces on the coils of the magnet. Our studies[39] indicate the separation between chamber and shield may be as large as 10 m. At this distance with the nominal field at 30 kG, we find the change in B_z is much less than 0.1%. The total force imbalance is $\sim$ 1300 lbs. on both coils, $\sim$ 1/20 of the safety limit.[40]

Another aspect of the question involves how many regenerated muons produced in the iron will strike the chamber. We have written a Monte Carlo program to simulate inclusive charged-current interactions and find that with the present 400 GeV beam in its current configuration and 10^{13} ppp, two muons are expected from the magnet coils and five or six from the earth beam. With the steel shield 10 meters from the chamber, the total muon counts become:

400 GeV	32 μ's/pulse
125 GeV	16 μ's/pulse .

These numbers are reduced to 10 and 6, respectively, by magnetizing the last 10 meters to the shield. We would propose to indeed do that, so that the muon background would not be increased.

C. <u>Comparison with e^+e^- Storage Ring Experiments</u>

One of the aims of the proposed experiment is the study of the branching ratios and spectroscopy of charmed baryons. For this particular aspect of the proposal, it is of interest to estimate the possible competition from results which might be obtained from e^+e^- annihilations to hadrons. At the present time, there are only some preliminary upper limits[41] to charmed baryon production in e^+e^- interactions. In this section, we review some theoretical estimates of charmed baryons production and compare them with these

reported upper limits.

For reasonable estimates of the charmed baryon masses, the ratio

$$R = \sigma(e^+e^- \to \text{hadrons})/\sigma(e^+e^- \to \mu^+\mu^-)$$

suggests[42] that there may be as much as 5% production of charmed baryons for cm energies $E_{cm} \gtrsim 5$ GeV (see Fig. 14a). A detailed calculation by Körner and Kuroda[43] based on the behavior of form factors for baryon production in the space-like region suggests by extension to the time-like region that charmed and uncharmed baryon production could be comparable fractions of the total hadronic cross sections just above their respective thresholds (i.e., the ratio $\sigma_{C\bar{C}}/\sigma_T$ close to $q^2_{C\bar{C}}$ threshold is comparable to $\sigma_{p\bar{p}}/\sigma_T$ close to $q^2_{p\bar{p}}$ threshold). In Fig. 14b, we show their results and note that the peak cross section constitutes about 0.5 nb (i.e., ~ 2.5% of the total hadronic cross section of ~ 20 nb). These large cross sections for $C\bar{C}$ production are expected[43] to be due to the form factor enhancement effects of close-by heavy $c\bar{c}$-vector meson states.

If we assume a similar cross section near 4.5 GeV for $M(C_0^+) = 2.25$ GeV, we can estimate the number of events that a "typical" experiment at either SPEAR or Cornell might expect to find.

(a) Cornell: From the design report (1977), we find that the peak design luminosity $\mathcal{L}_{pk}$ is the following function of the beam energy E_o:

$$\mathcal{L}_{pk} = 10^{32} \left(\frac{E_o}{8}\right)^2 \text{cm}^{-2}\,\text{sec}^{-1} \quad .$$

Assuming an average luminosity over an experiment is $\mathcal{L} = \frac{1}{4}\mathcal{L}_{pk}$, we find that for $E_{cm} = 4.5$ GeV, $\mathcal{L} = 2.0 \times 10^{30}$ cm^{-2} sec^{-1}.

(b) SPEAR: The luminosity at SPEAR is given by $\mathcal{L} = 10^{31}\left(\frac{E_o}{3.5}\right)^4$ which yields $\mathcal{L} = 1.7 \times 10^{30}$ cm^{-2} sec^{-1} at $E_{cm} = 4.5$ GeV. Thus the rates at SPEAR and Cornell are quite similar for $E_o = 2.25$ GeV.

Let us assume that a typical run yields 30,000 hadronic events. This corresponds to an integrated luminosity of 1500 nb^{-1}. Then for a production cross section of 0.5 nb, this yields a total of 750 C_0^+ events. This is a factor of five smaller than the number we might expect in the ν proposal. At higher beam energies, the e^+e^- luminosities are increasing slowly; this is offset, however, by the rapidly decreasing exclusive cross sections and even fewer events would be expected. Hence, it appears that our proposed ν experiment is very competitive with the e^+e^- storage ring experiments at both SPEAR and Cornell.

Finally, it is interesting to compare these theoretical predictions with the upper limits recently reported[41] at the Washington APS meeting:

$$\sigma \cdot BR(C_0^+ \to \Lambda\pi^+) < 4 \text{ pb}$$

$$\sigma \cdot BR(C_0^+ \to \Lambda\pi^+\pi^+\pi^-) < 10 \text{ pb}$$

at 95% CL for $5.8 \leq E_{cm} \leq 7.4$ GeV with $\langle E_{cm} \rangle \sim 6.8$ GeV. We first have to make some estimate of the branching ratios for $\Lambda\pi$, $\Lambda 3\pi$:

$$\left(\frac{C_0^+ \to \Lambda\pi^+\pi^+\pi^-}{C_0^+ \to \text{all}}\right) = \left(\frac{\Lambda\pi^+\pi^+\pi^-}{\Lambda 3\pi}\right)\left(\frac{\Lambda 3\pi}{\Lambda m\pi}\right)\left(\frac{\Lambda m\pi}{\text{had.}}\right)\left(\frac{\text{had.}}{\text{all}}\right)$$

$$\text{Ref. 11} \quad \text{Ref. 10}$$

$$= (\leq 0.8)(0.28)(\tfrac{2}{3} \times \tfrac{2}{3})(\leq 0.9) \leq 0.09$$

and

$$\left(\frac{C_0^+ \to \Lambda\pi^+}{C_0^+ \to \text{all}}\right) = \left(\frac{\Lambda\pi^+}{\Lambda m\pi}\right)\left(\frac{\Lambda m\pi}{\text{had.}}\right)\left(\frac{\text{had.}}{\text{all}}\right) \overset{\text{Ref. 10}}{=} (0.18)(\tfrac{2}{3} \times \tfrac{2}{3})(\leq 0.9) \leq 0.072 \ ,$$

so that $\sigma(C_0^+ \text{ at } 6.8 \text{ GeV}) < 4/0.072 = 55.6$ pb

or $\sigma(C_0^+ \text{ at } 6.8 \text{ GeV}) < 10/0.90 = 111$ pb

at the 95% CL, whereas in Fig. 14b, the exclusive $C_0\bar{C}_0$ cross section is predicted to be of order 4pb at 6.8 GeV. Hence, at the current time, it appears that the SPEAR results are not in conflict with the theory of Körner and Kuroda.

D. Comparison with Photoproduction Experiments

With regard to theoretical predictions of the cross sections for the photoproduction of charmed baryons, Sivers et al.[44] using an inequality based on unitarity derive the following lower limit:

$$\sigma(\gamma p \rightarrow D\overline{D} + \text{anything}) \geqslant 300 \text{ nb} \quad , \tag{36}$$

where the D's are any mesons or baryons containing charmed quarks.

With regard to the experimental situation, there is the published result of Knapp et al.[45] which suggests the existence of the $\overline{C}_0^-(2260)$ with an estimated[46] cross section times branching ratio of

$$\sigma \cdot BR(\overline{C}_0 \rightarrow \overline{\Lambda}\pi^-\pi^-\pi^+) \sim 1 - 10 \text{ nb}$$

integrated over the broad band photon peak spectrum. Again, using a 9% rate for $C_0^+ \rightarrow \Lambda\pi^+\pi^+\pi^-$ with a visible Λ decay, this yields $\sigma(\gamma p \rightarrow \overline{C}_0^- + \text{anything}) = 10 - 100$ nb. This would not appear to conflict with Eq. (36) since the latter contains $\psi, D, D^* \ldots$ production cross sections in addition to other heavier mass charmed baryons.

In order to use this result to estimate the competition between our proposal and the photoproduction experiment, we can quote the results from Fermilab proposal P-516.[47] Scaling the event rates given in their Table I to the 10-100 nb $\overline{C}_0^+(2260)$ cross section, if their acceptance is only 1%, they would get 3,000-30,000 $\overline{C}_0^+$ events in 1000 hours of running. These numbers are similar to the 4,000 C_0^+ events we have estimated in our Table I. It would seem, therefore, that in terms of statistics, the two experiments are quite comparable. There are, however, two effects which could favor the ν production over the photoproduction experiments:

(a) In P-516, it is noted that the broad band beam fluxes are significantly greater than the proposed tagged photon fluxes for energies $E_\gamma \gtrsim 150$

GeV. If a significant fraction of the events of Knapp et al. are produced at the highest energies, then the above-estimated number of photoproduction events expected would be lowered accordingly.

(b) As shown in Ref. 7, the $\overline{C}_0$ is produced with a large amount of background. It would appear quite likely that the lower energy ν-production of $C_0(2260)$ could show much less background. This would be of particular importance in measuring the properties of the charmed baryons.

APPENDIX II

Possible Extensions of the Proposed Beam

II.A A Possible High Flux ν_e, $\bar{\nu}_e$ Beam

The advantages of the increased solid angle discussed so far only for ν_μ production from $\pi \to \mu\nu$ also carry over to ν_e, $\bar{\nu}_e$ production from $K_L^o \to \pi e \nu$ decays. This source of ν_e, $\bar{\nu}_e$ has already been discussed by Baltay et al. in P-296, using the existing beam line. The interesting and important new range of weak interaction physics opened up by having such a beam is stressed in P-296.

For a proton energy of 400 GeV, the shorter beam line proposed here would allow more than an order of magnitude increase in the ν_e, $\bar{\nu}_e$ flux, extending over a substantial range of neutrino energy. However, the problems of reducing the background of ν_μ from high energy $\pi, K \to \mu\nu$ and of eliminating high energy muons from $K_L^o \to \pi\mu\nu_\mu$ decays, which can easily penetrate the 75 m iron shield, are made more severe.

The essential design details for the K_L^o beam are described in P-296 and their proposal for removing $\pi^\pm$, $K^\pm$, and $K_s^o \to \pi^+\pi^-$ from the beam would be adopted here. Modifications would be needed to the target enclosure to provide space and utilities for the sweeping magnet train. In P-296, this consists of 5 m - 40 kG magnet containing a 2-1/2 mrad collimator immediately following the target, then a series of magnets equivalent to 40 m - 10 kG to remove π from $K_s^o \to 2\pi$. While the sweeping is adequate to stop all charged particles originating within this magnetic volume from reaching the chamber, the increased solid angle of this beam over that considered in P-296 also implies a larger collimator angle than used in P-296. The ν_μ background at the chamber from $\pi^\pm, K^\pm$ decays near the target is then increased.

The μ from $K_L^o \rightarrow \pi \mu \nu_\mu$ will extend in momentum up to that of the proton beam. One way to exclude them from the chamber is to introduce magnetized iron after the drift space. The location of the 75 m shield in Fig. 2 provides too short a lever arm for any reasonable magnetization. One solution would be to introduce ~ 45 m of magnetized iron in front of the proposed 75 m shield. With careful design, a field of 15 kG would be obtained.

Whether or not this very substantial gain in studying ν_e, $\bar{\nu}_e$ interactions can be realized obviously rests on a detailed study of these problems. However, one can anticipate substantial interest from users in developing such a potential.

II. B Narrow Band Beams

A short narrow-band beam is possible using the proposed drift and shield lengths. As an example, imposing a momentum bite $13 < p < 18$ GeV/c on the mesons focussed by the horns of the standard beam gives a neutrino flux concentrated between 3 and 6 GeV and peaking at 5 GeV. The peak flux is one-half as large as the broad-band flux at 5 GeV, and the overall event rate is one-tenth that of the broad-band beam. The narrow-band peak from kaon decays is only 3% of the flux and 10% of the total event rate in this beam.

There is some correlation of neutrino energy and position in the bubble chamber, and the effective width of the neutrino spectrum is therefore somewhat less than 3 GeV. The meson momentum bite could be further reduced with a direct tradeoff between neutrino energy bite and event rate. The prospect of four-constraint event fitting and some one-constraint ambiguity resolution is attractive. While we do not propose to build such a beam ourselves, it is a possibility, which some other potential users of this facility may wish to consider, for use with the neon-hydrogen 15-foot chamber or with some possible large electronic detectors.

One possible design for such a beam could be the Baltay dichromatic horn configuration as appended to P-380, suitably scaled down in energy.

Appendix III

Recognizing Semi Leptonic Decays of the C_0^+ in Deuterium

In isolating the reaction

$$\nu n \to \mu^- C_0^+ \quad \llcorner \Lambda e^+ \nu \tag{37}$$

one must eliminate a large background of associated production events from reactions such as

$$\left.\begin{array}{l} \nu n \to \mu^- \Lambda^o K^+ \pi^o \\ \qquad\quad \mu^- \Lambda^o \pi^+ K^o \\ \nu n \to \mu^- C_0^+ \\ \qquad\quad \llcorner \Lambda^o \pi^+ \end{array}\right\} \tag{38}$$

Reaction (37) involves four unknown quantities: the energy of the incident neutrino and the three momentum components of the decay neutrino. While the conservation of four-momentum allows one to determine these quantities the equations are not overconstrained. Nevertheless, the resolution on the effective mass of the $\Lambda^o e^+ \nu$ is approximately ± 35 MeV. This is already likely to be sufficiently good to isolate reaction (37).

If in addition there is μ and e identification, the isolation of reaction (37) will be quite straight forward. This can be done by using the external muon identifier (E. M. I) and by having a set of high Z metal plates in the bubble cahmber (see Fig. 15).

A Monte Carlo study of reaction (37) has been carried out using the following model. The Q^2 dependence of the C_0^+ production was assumed to have a dipole form and a characteristic mass of 1.5 GeV. (Masses of 1 and 2 GeV were also tried and were found not to substantially alter the results given below.) The decay of the C_0^+ was assumed to follow simple three body phase space.

We find that 80% of the μ^- tracks from these events would hit the EMI as presently configured. For the e^+, we find that 40% of events occuring upstream of the plates will have an electron which intersects the plates. Hence approximately 1/3 of these dilepton events will be recognized by using the EMI and internal plates.

In addition to electrons identified by the plates others will be recognized which either lose substantial energy through Bremsstraulung or have characteristically high energy δ rays. We estimate that approximately 30% of the electrons missing the plates could be recognized in the deuterium filled 15-foot bubble chamber. Thus a total of nearly 50% of the μe dileptons from reaction (37) would be identified in the D_2- filled bubble chamber with plates.

References

1. We thank Professor L. Wolfenstein and Dr. John Babcock for helpful discussions.
2. J. Campbell et al., Phys. Rev. Letters 30, 335 (1973).
3. C. L. Wang, Phys. Rev. D10, 3876 (1974).
4. W. F. Baker et al., Phys. Letters 51B, 303 (1974).
5. J. Cooper et al., Nucl. Physics B80, 239 (1974).
6. The Fermilab Neutrino Flux Program by D. C. Carey and V. A. White.
7. R. E. Shrock and B. W. Lee, Phys. Rev. D13, 2539 (1976).
8. C. Avilez, T. Koboyashi and J. G. Korner, "Quark Model Calculations of Charmed Baryon Production by Neutrinos," DESY Preprint 76161, November 1976.
9. G. Kopp, L. M. Sehgal, P. M. Zerwas, "Neutrino Excitation of $C_0^+(2260)$ and Tests of the Charmed Current Structure," Aachen preprint, December 1976.
10. B. W. Lee, C. Quigg, and J. L. Rosner, Phys. Rev. D15, 157 (1977).
11. M. Peshkin and J. L. Rosner, COO 2200-93 (December 1976), to be published in Nuclear Physics B.
12. A. Buras and J. Ellis, Nucl. Phys. B111, 341 (1976).
13. G. Kopp, L. M. Sehgal, and P. M. Zerwas, "Λ Polarization in Neutrino-Induced $\mu e \Lambda$ Events," Aachen preprint, January 1977.
14. H. Deden et al., "Dilepton and Strange Particle Production by Neutrinos in Gargamelle," CERN preprint/EP/Phys. 77-2, January 1977, submitted to Phys. Letters B. These authors look for and identify Λe^+ events and estimate total baryon charm from excess of Λ's over what is expected associated production. This gives

$$BR \frac{C \to (\Lambda^o + e^+ + \ldots)}{C \to (\Lambda^o + \text{anything})} = (15 \begin{smallmatrix} +8 \\ -7 \end{smallmatrix})\% \quad .$$

Another measure of associated production is provided by the Gargamelle result 22 $\Lambda^o K^+ \ldots$, (42 ± 20) unassociated Λ^o's.

15. H. Deden et al., Nucl. Phys. B85, 269 (1975). Also see D. H. Perkins, "Topics in Lepton-Hadron Interactions," ANL-HEP-76-54.

16. S. J. Barish et al., Phys. Letters 66B, 291 (1977).

17. D. Bloess et al., Nucl. Instruments and Methods 91, 605 (1971).

18. S. Adler, Phys. Rev. 143, 1144 (1966).

19. D. J. Gross and C. H. Llewellyn-Smith, Nucl. Phys. B14, 337 (1969).

20. D. Cline, "Inelastic Neutrino and Antineutrino Scattering from Hadrons," Rapporteurs Report at the International Conference on High Energy Physics, Palermo, Sicily.

21. B. R. Holstein and S. B. Treiman, Phys. Rev. D13, 3059 (1976).

22. S. Adler, Phys. Rev. 135, 963 (1965).

23. S. V. Bonetti et al., Nuovo Cimento Letters, Vol. II, No. 18, 877 (1969).

24. G. Farrar, CALT-69-589 (1977).

25. J. Campbell et al., Phys. Rev. Letters 30, 335 (1973); A. Mann et al., Phys. Rev. Letters 31, 844 (1973); S. J. Barish et al., Phys. Rev. Letters 36, 179 (1976).

26. P. A. Schreiner and F. Von Hippel, Nucl. Phys. B58, 333 (1973).

27. P. Zucker, Phys. Rev. D4, 3350 (1971).

28. E. Monsay, Ph.D. Thesis, Princeton University (1977).

29. C. Llewellyn-Smith, Physics Reports 3C, 261 (1972).

30. M. S. Chen et al., Nucl. Phys. B118, 345 (1977).

31. M. K. Gaillard et al., Nucl. Phys. B102, 326 (1976). Erratum, Nucl.

Phys. B112, 545 (1976). See also "Diffractive Neutrino Production of Vector Mesons," M. K. Gaillard and C. A. Piketty, preprint LEPENS 77/5.

32. D. H. Perkins, "Review of Neutrino Experiments," Proceedings of the 1975 International Symposium on Lepton and Photon Interactions at High Energies, Stanford University.

33. E31 $\bar{\nu}$ - H_2; E45 ν -H_2; E151 ν - D_2; E390 $\bar{\nu}$ - D_2.

34. Hung and J. J. Sakurai, Phys. Letters 63B, 295 (1976).

35. L. Wolfenstein and D. Wyler, Carnegie-Mellon Preprint COO-3066-77.

36. J. Mapp, private communication on E-28.

37. C. Baltay, private communication on E-53.

38. Amalio Fernandez-Pacheco and J. A. Grifols, SLAC-PUB-1899 (1977).

39. We thank R. Lari of the ARF Division, ANL for doing these calculations.

40. Private communication from G. Mulholland.

41. D. Luke et al., Paper BK9, Washington APS Meeting (1977).

42. A. DeRujula et al., Phys. Rev. Letters 37, 785 (1976).

43. J. C. Körner and M. Kuroda, DESY preprint 76/34 (1976).

44. D. Sivers et al., Phys. Rev. D13, 1234 (1976).

45. B. Knapp et al., Phys. Rev. Letters 37, 882 (1976).

46. J. Peoples, private communication.

47. FNAL Proposal No. 516, "Proposal to Study Photoproduction of final States of Mass Above 2.5 GeV with a Magnetic Spectrometer in the Tagged Photon Lab," T. Nash, Spokesperson (October 1976).

Table I

Event Totals for 125 and 400 GeV Protons

Assumes 10^{19} protons on target, a 18.7 m^3 detector fiducial volume, and $\rho_{D_2} = 0.12$ gm cm^{-3}.

Reaction	125 GeV	400 GeV
$\nu + n \rightarrow \mu^- + C_0^+$	4,100	1,050
$\nu + p \rightarrow \mu^- + C_1^{++}$	750	210
$\nu + n \rightarrow \mu^- + C_1^+$	380	110
$\nu + p \rightarrow \mu^- + C_1^{*++}$	920	250
$\nu + n \rightarrow \mu^- + C_1^{*+}$	450	130
Total of above 5	6,600	1,750
$\nu + p \rightarrow \mu^- + \Delta^{++}$	13,500	1,200
Total Inclusive Charged Current	210,000	124,550
Total Inclusive Charm Production*	14,000	9,300

*This assumes charm production is 7.5% of the total inclusive charged current rate.

Table II

ν-D_2 Charged and Neutral Current Inclusive Rates
(For 10^{19} protons on target; fiducial volume 18.7 m^3)

E_ν GeV	Total Events	Total Charged Current Events*		Total Neutral Current Events+
2 - 4	25,000	20,000	(7600)‡	5,000
4 - 6	43,400	42,700	(2200)	10,700
6 - 8	41.450	33,150	(1100)	8,300
8 - 10	29,450	23,550	(770)	5,900
10 - 15	41,000	32,800	(740)	8,200
15 - 20	21,000	16,900		4,200
20 - 30	25,050	20,050		5,000
30 - 45	15,500	13,200		3,300
45 - 60	5,050	4,050		1,000

*Assume $\sigma(E_\nu) = 0.74\, E_\nu \cdot 10^{-38}$ cm^2/nucleon/GeV

+Assume $\sigma_{NC} = 0.25\, \sigma_{CC}$.

‡Numbers in parentheses refer to an exposure of 10^{19} protons on target using the 7-foot BNL chamber with a fiducial volume 5.5 m^3. The proton energy is 35 GeV.

Table III

Some Exclusive Final State Rates in ν-D_2 for 10^{19} Protons on Target

E_ν GeV	$\mu^- p^+$	$\mu^- p\pi^+$ *	$\mu^- p\pi^+\pi^-$ *	$\mu^- p\pi^+\pi^-\pi^+$ ‡ $\mu^- p\pi^+\pi^-\pi^o$ $\mu^- n\pi^+\pi^+\pi^-$
2.0 - 4.0	2330	3260	3260	4660
4.0 - 6.0	2990	4190	4190	5980
6.0 - 8.0	1600	2240	2240	3200
8.0 - 10.0	870	1220	1220	1740
10.0 - 15.0	915	1280	1280	1830
15.0 - 20.0	340	475	475	680
20.0 - 30.0	280	390	390	560
Total	9,325	13,055	13,055	18,650

All assume a constant cross section.

$^+\sigma = 0.5 \times 10^{-38}\ cm^2$

$^*\sigma = 0.7 \times 10^{-38}\ cm^2$

$^‡\sigma = 1.0 \times 10^{-38}\ cm^2$

Table IV

Reaction	Events
$\nu n \to \mu^- N^{*+}(1520)$	1750
$\nu n \to \mu^- N^{*+}(1688)$	850
$\nu p \to \mu^- \Delta^{++}(1236)$	13000

Table V

g_{II}	σ(2 GeV) $10^{-38}cm^2$	Events 1.75 - 2.25 GeV	σ(6 GeV) $10^{-38}cm^2$	Events 5.75 - 6.25 GeV
0	0.49	325	0.51	675
$-6F_A(0)$	0.925	650	1.37	1750

Table VI

Reaction	No. of Events+	No. of Events*
$\nu + p \to \mu^- \rho^+ p$	125	1300
$\nu + p \to \mu^- A_1^+ p$	50	3000
$\nu + p \to \mu^- F^{*+} p$		~100

All the above tables are calcuated for standard exposure of 10^{19} protons.

+The event rate is calculated using the cross section given in Ref. 30.

*This rates use the result of Ref. 31.

Figure Captions

Fig. 1 Charmed baryon cross sections from Ref. 8.

Fig. 2 125 GeV proton beam layout and overlay.

Fig. 3 Some typical K^+ and π^+ yields at 102 GeV/c. The line represents the Wang parameterization.

Fig. 4 ν flux at 125 GeV and 400 GeV.

Fig. 5 $\bar{\nu}$ flux at 125 GeV.

Fig. 6 Main ring cycle for dedicated ν running.

Fig. 7 The effective mass for events generated as $C_0^+ \to \Lambda\pi^+\pi^+\pi^-$ with the misidentified background from associated production.

Fig. 8 Various distributions for $C_0^+ \to \Lambda e^+\nu$ decay:

(a) The normalized $(\Lambda^o e)$ effective mass distribution with $M_{C_0^+}$ = 2.5 GeV and M_{F^*} = 2.2 GeV.

(b) The dependence of $< M(\Lambda e^+) >$ on the mass $M_{C_0^+}$ for various choices of coupling.

(c) The dependence of $< E_{e^+} >$ on $M_{C_0^+}$ for various choice of coupling.

Fig. 9 For the process $C_0^+ \to \Lambda e^+\nu$:

(a) The polarization vector $\hat{\pi}_{B_f}$ for various choices of the couplings.

(b) The projected distributions for the reaction $C_0^+ \to \Lambda e^+\nu$ for different choice of couplings.

Fig. 10 Monte Carlo simulations of the projected distributions in the $C_0^+ \to \Lambda e^+\nu$ decay.

Fig. 11 The expected hadronic mass (W) distribution in inclusive νp charged-current interactions: (a) for all Q^2, (b) for $Q^2 > 1.0\ \mathrm{GeV}^2$.

Fig. 12 The Q^2 distribution for νp interactions.

Fig. 13 The differential cross section for $\nu n \rightarrow \mu^- p$ for various strengths of the second class current form factor.

Fig. 14 (a) Limit on the charmed baryon contribution to $R = \sigma(e^+e^- \rightarrow \text{hadron})/\sigma(e^+e^- \rightarrow \mu^+\mu^-)$; (b) cross section for C_0^+ production in e^+e^- collisions.

Fig. 15 Possible plate arrangement for the 15-foot bubble chamber.

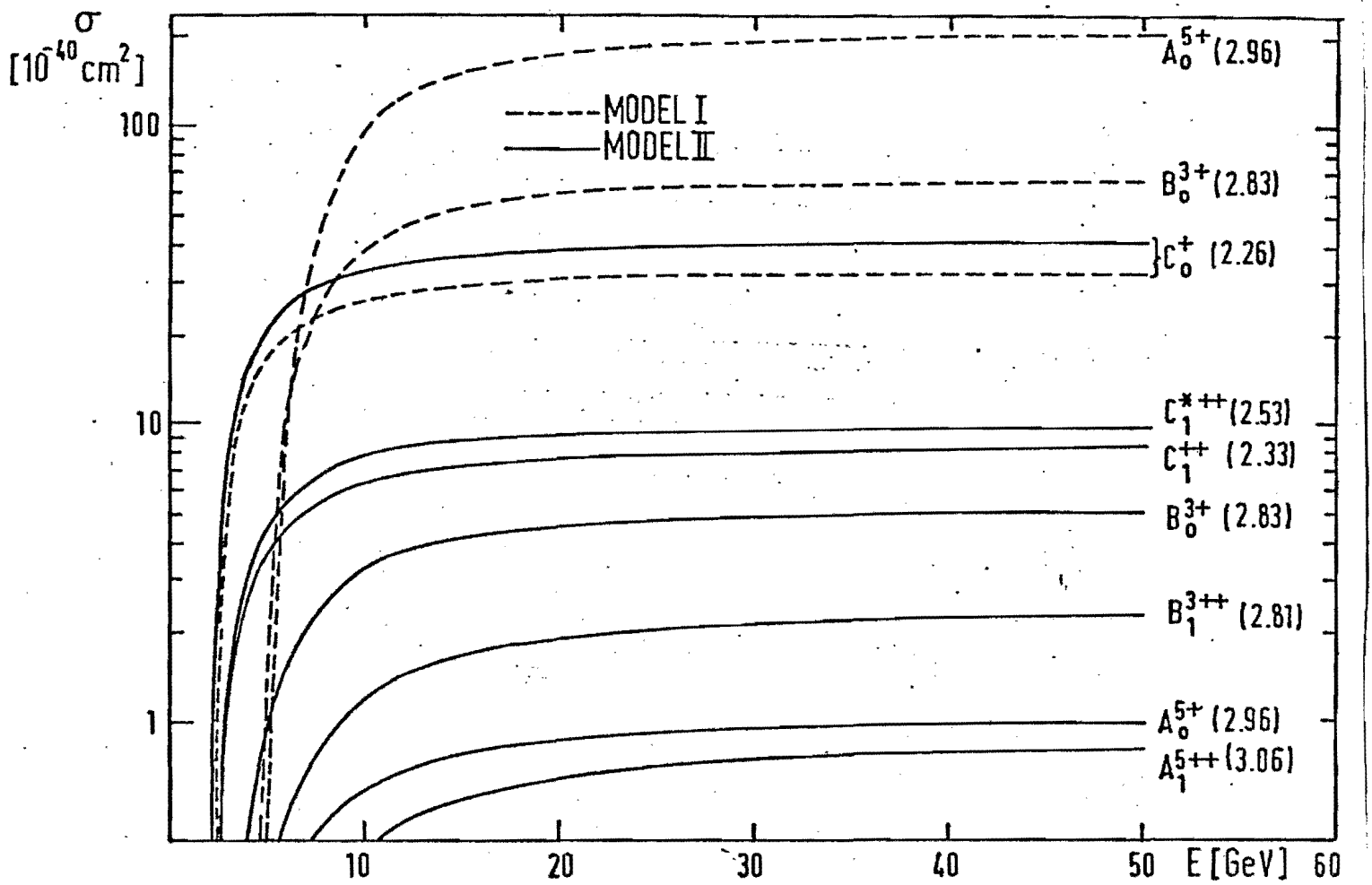
σ
[10^-40 cm^2]
100
10
1
MODEL I
MODEL II
A_o^5+ (2.96)
B_o^3+ (2.83)
C_o^+ (2.26)
C_1^*++ (2.53)
C_1^++ (2.33)
B_o^3+ (2.83)
B_1^3++ (2.81)
A_o^5+ (2.96)
A_1^5++ (3.06)
10
20
30
40
50
E [GeV]
60

Fig./1

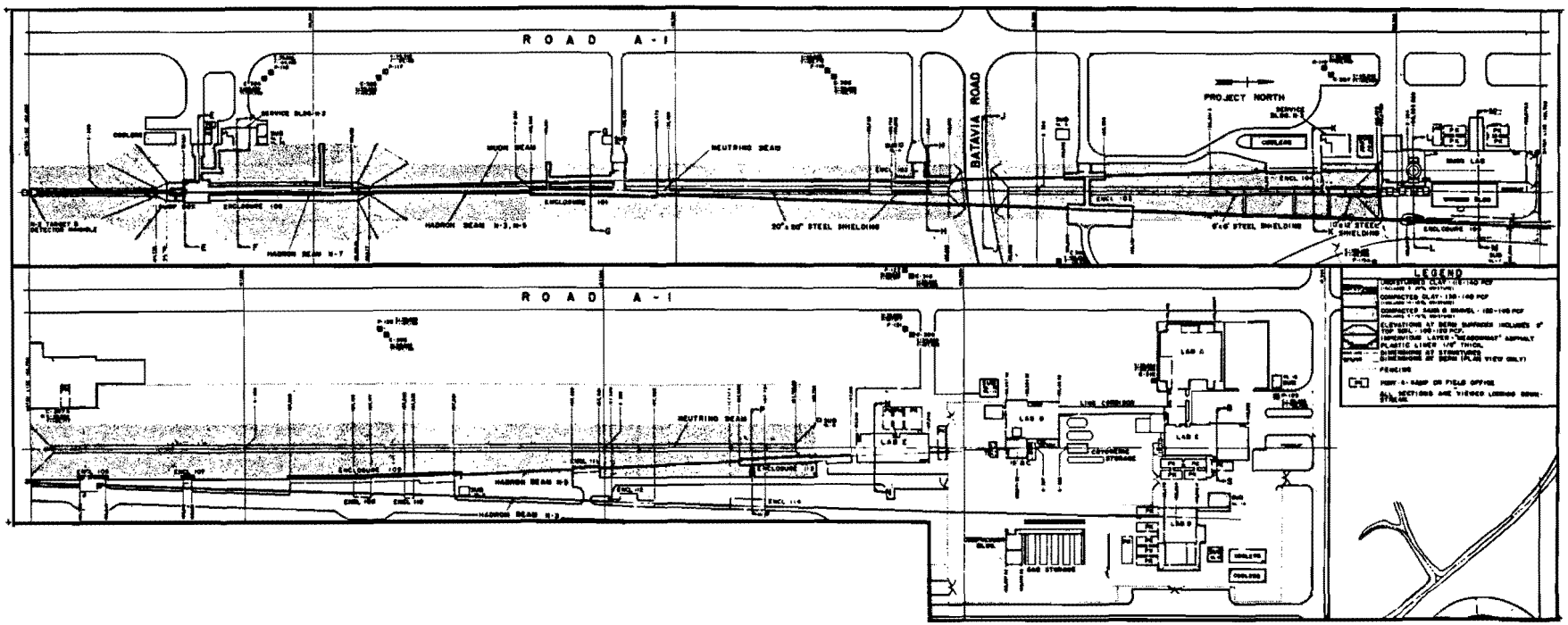
ROAD A-1
BATAVIA ROAD
PROJECT NORTH
NEUTRINO BEAM
HADRON BEAM
ENCLOSURE 100
ENCLOSURE 101
ENCLOSURE 102
ENCLOSURE 103
ENCLOSURE 104
ENCLOSURE 105
ENCLOSURE 106
ENCLOSURE 107
ENCLOSURE 108
ENCLOSURE 109
ENCLOSURE 110
ENCLOSURE 111
ENCLOSURE 112
ENCLOSURE 113
ENCLOSURE 114
ENCL 115
ENCL 116
ENCL 117
ENCL 118
ENCL 119
ENCL 120
ENCL 121
ENCL 122
ENCL 123
ENCL 124
ENCL 125
ENCL 126
ENCL 127
ENCL 128
ENCL 129
ENCL 130
ENCL 131
ENCL 132
ENCL 133
ENCL 134
ENCL 135
ENCL 136
ENCL 137
ENCL 138
ENCL 139
ENCL 140
ENCL 141
ENCL 142
ENCL 143
ENCL 144
ENCL 145
ENCL 146
ENCL 147
ENCL 148
ENCL 149
ENCL 150
ENCL 151
ENCL 152
ENCL 153
ENCL 154
ENCL 155
ENCL 156
ENCL 157
ENCL 158
ENCL 159
ENCL 160
ENCL 161
ENCL 162
ENCL 163
ENCL 164
ENCL 165
ENCL 166
ENCL 167
ENCL 168
ENCL 169
ENCL 170
ENCL 171
ENCL 172
ENCL 173
ENCL 174
ENCL 175
ENCL 176
ENCL 177
ENCL 178
ENCL 179
ENCL 180
ENCL 181
ENCL 182
ENCL 183
ENCL 184
ENCL 185
ENCL 186
ENCL 187
ENCL 188
ENCL 189
ENCL 190
ENCL 191
ENCL 192
ENCL 193
ENCL 194
ENCL 195
ENCL 196
ENCL 197
ENCL 198
ENCL 199
ENCL 200
ENCL 201
ENCL 202
ENCL 203
ENCL 204
ENCL 205
ENCL 206
ENCL 207
ENCL 208
ENCL 209
ENCL 210
ENCL 211
ENCL 212
ENCL 213
ENCL 214
ENCL 215
ENCL 216
ENCL 217
ENCL 218
ENCL 219
ENCL 220
ENCL 221
ENCL 222
ENCL 223
ENCL 224
ENCL 225
ENCL 226
ENCL 227
ENCL 228
ENCL 229
ENCL 230
ENCL 231
ENCL 232
ENCL 233
ENCL 234
ENCL 235
ENCL 236
ENCL 237
ENCL 238
ENCL 239
ENCL 240
ENCL 241
ENCL 242
ENCL 243
ENCL 244
ENCL 245
ENCL 246
ENCL 247
ENCL 248
ENCL 249
ENCL 250
ENCL 251
ENCL 252
ENCL 253
ENCL 254
ENCL 255
ENCL 256
ENCL 257
ENCL 258
ENCL 259
ENCL 260
ENCL 261
ENCL 262
ENCL 263
ENCL 264
ENCL 265
ENCL 266
ENCL 267
ENCL 268
ENCL 269
ENCL 270
ENCL 271
ENCL 272
ENCL 273
ENCL 274
ENCL 275
ENCL 276
ENCL 277
ENCL 278
ENCL 279
ENCL 280
ENCL 281
ENCL 282
ENCL 283
ENCL 284
ENCL 285
ENCL 286
ENCL 287
ENCL 288
ENCL 289
ENCL 290
ENCL 291
ENCL 292
ENCL 293
ENCL 294
ENCL 295
ENCL 296
ENCL 297
ENCL 298
ENCL 299
ENCL 300
ENCL 301
ENCL 302
ENCL 303
ENCL 304
ENCL 305
ENCL 306
ENCL 307
ENCL 308
ENCL 309
ENCL 310
ENCL 311
ENCL 312
ENCL 313
ENCL 314
ENCL 315
ENCL 316
ENCL 317
ENCL 318
ENCL 319
ENCL 320
ENCL 321
ENCL 322
ENCL 323
ENCL 324
ENCL 325
ENCL 326
ENCL 327
ENCL 328
ENCL 329
ENCL 330
ENCL 331
ENCL 332
ENCL 333
ENCL 334
ENCL 335
ENCL 336
ENCL 337
ENCL 338
ENCL 339
ENCL 340
ENCL 341
ENCL 342
ENCL 343
ENCL 344
ENCL 345
ENCL 346
ENCL 347
ENCL 348
ENCL 349
ENCL 350
ENCL 351
ENCL 352
ENCL 353
ENCL 354
ENCL 355
ENCL 356
ENCL 357
ENCL 358
ENCL 359
ENCL 360
ENCL 361
ENCL 362
ENCL 363
ENCL 364
ENCL 365
ENCL 366
ENCL 367
ENCL 368
ENCL 369
ENCL 370
ENCL 371
ENCL 372
ENCL 373
ENCL 374
ENCL 375
ENCL 376
ENCL 377
ENCL 378
ENCL 379
ENCL 380
ENCL 381
ENCL 382
ENCL 383
ENCL 384
ENCL 385
ENCL 386
ENCL 387
ENCL 388
ENCL 389
ENCL 390
ENCL 391
ENCL 392
ENCL 393
ENCL 394
ENCL 395
ENCL 396
ENCL 397
ENCL 398
ENCL 399
ENCL 400
ENCL 401
ENCL 402
ENCL 403
ENCL 404
ENCL 405
ENCL 406
ENCL 407
ENCL 408
ENCL 409
ENCL 410
ENCL 411
ENCL 412
ENCL 413
ENCL 414
ENCL 415
ENCL 416
ENCL 417
ENCL 418
ENCL 419
ENCL 420
ENCL 421
ENCL 422
ENCL 423
ENCL 424
ENCL 425
ENCL 426
ENCL 427
ENCL 428
ENCL 429
ENCL 430
ENCL 431
ENCL 432
ENCL 433
ENCL 434
ENCL 435
ENCL 436
ENCL 437
ENCL 438
ENCL 439
ENCL 440
ENCL 441
ENCL 442
ENCL 443
ENCL 444
ENCL 445
ENCL 446
ENCL 447
ENCL 448
ENCL 449
ENCL 450
ENCL 451
ENCL 452
ENCL 453
ENCL 454
ENCL 455
ENCL 456
ENCL 457
ENCL 458
ENCL 459
ENCL 460
ENCL 461
ENCL 462
ENCL 463
ENCL 464
ENCL 465
ENCL 466
ENCL 467
ENCL 468
ENCL 469
ENCL 470
ENCL 471
ENCL 472
ENCL 473
ENCL 474
ENCL 475
ENCL 476
ENCL 477
ENCL 478
ENCL 479
ENCL 480
ENCL 481
ENCL 482
ENCL 483
ENCL 484
ENCL 485
ENCL 486
ENCL 487
ENCL 488
ENCL 489
ENCL 490
ENCL 491
ENCL 492
ENCL 493
ENCL 494
ENCL 495
ENCL 496
ENCL 497
ENCL 498
ENCL 499
ENCL 500
ENCL 501
ENCL 502
ENCL 503
ENCL 504
ENCL 505
ENCL 506
ENCL 507
ENCL 508
ENCL 509
ENCL 510
ENCL 511
ENCL 512
ENCL 513
ENCL 514
ENCL 515
ENCL 516
ENCL 517
ENCL 518
ENCL 519
ENCL 520
ENCL 521
ENCL 522
ENCL 523
ENCL 524
ENCL 525
ENCL 526
ENCL 527
ENCL 528
ENCL 529
ENCL 530
ENCL 531
ENCL 532
ENCL 533
ENCL 534
ENCL 535
ENCL 536
ENCL 537
ENCL 538
ENCL 539
ENCL 540
ENCL 541
ENCL 542
ENCL 543
ENCL 544
ENCL 545
ENCL 546
ENCL 547
ENCL 548
ENCL 549
ENCL 550
ENCL 551
ENCL 552
ENCL 553
ENCL 554
ENCL 555
ENCL 556
ENCL 557
ENCL 558
ENCL 559
ENCL 560
ENCL 561
ENCL 562
ENCL 563
ENCL 564
ENCL 565
ENCL 566
ENCL 567
ENCL 568
ENCL 569
ENCL 570
ENCL 571
ENCL 572
ENCL 573
ENCL 574
ENCL 575
ENCL 576
ENCL 577
ENCL 578
ENCL 579
ENCL 580
ENCL 581
ENCL 582
ENCL 583
ENCL 584
ENCL 585
ENCL 586
ENCL 587
ENCL 588
ENCL 589
ENCL 590
ENCL 591
ENCL 592
ENCL 593
ENCL 594
ENCL 595
ENCL 596
ENCL 597
ENCL 598
ENCL 599
ENCL 600
ENCL 601
ENCL 602
ENCL 603
ENCL 604
ENCL 605
ENCL 606
ENCL 607
ENCL 608
ENCL 609
ENCL 610
ENCL 611
ENCL 612
ENCL 613
ENCL 614
ENCL 615
ENCL 616
ENCL 617
ENCL 618
ENCL 619
ENCL 620
ENCL 621
ENCL 622
ENCL 623
ENCL 624
ENCL 625
ENCL 626
ENCL 627
ENCL 628
ENCL 629
ENCL 630
ENCL 631
ENCL 632
ENCL 633
ENCL 634
ENCL 635
ENCL 636
ENCL 637
ENCL 638
ENCL 639
ENCL 640
ENCL 641
ENCL 642
ENCL 643
ENCL 644
ENCL 645
ENCL 646
ENCL 647
ENCL 648
ENCL 649
ENCL 650
ENCL 651
ENCL 652
ENCL 653
ENCL 654
ENCL 655
ENCL 656
ENCL 657
ENCL 658
ENCL 659
ENCL 660
ENCL 661
ENCL 662
ENCL 663
ENCL 664
ENCL 665
ENCL 666
ENCL 667
ENCL 668
ENCL 669
ENCL 670
ENCL 671
ENCL 672
ENCL 673
ENCL 674
ENCL 675
ENCL 676
ENCL 677
ENCL 678
ENCL 679
ENCL 680
ENCL 681
ENCL 682
ENCL 683
ENCL 684
ENCL 685
ENCL 686
ENCL 687
ENCL 688
ENCL 689
ENCL 690
ENCL 691
ENCL 692
ENCL 693
ENCL 694
ENCL 695
ENCL 696
ENCL 697
ENCL 698
ENCL 699
ENCL 700
ENCL 701
ENCL 702
ENCL 703
ENCL 704
ENCL 705
ENCL 706
ENCL 707
ENCL 708
ENCL 709
ENCL 710
ENCL 711
ENCL 712
ENCL 713
ENCL 714
ENCL 715
ENCL 716
ENCL 717
ENCL 718
ENCL 719
ENCL 720
ENCL 721
ENCL 722
ENCL 723
ENCL 724
ENCL 725
ENCL 726
ENCL 727
ENCL 728
ENCL 729
ENCL 730
ENCL 731
ENCL 732
ENCL 733
ENCL 734
ENCL 735
ENCL 736
ENCL 737
ENCL 738
ENCL 739
ENCL 740
ENCL 741
ENCL 742
ENCL 743
ENCL 744
ENCL 745
ENCL 746
ENCL 747
ENCL 748
ENCL 749
ENCL 750
ENCL 751
ENCL 752
ENCL 753
ENCL 754
ENCL 755
ENCL 756
ENCL 757
ENCL 758
ENCL 759
ENCL 760
ENCL 761
ENCL 762
ENCL 763
ENCL 764
ENCL 765
ENCL 766
ENCL 767
ENCL 768
ENCL 769
ENCL 770
ENCL 771
ENCL 772
ENCL 773
ENCL 774
ENCL 775
ENCL 776
ENCL 777
ENCL 778
ENCL 779
ENCL 780
ENCL 781
ENCL 782
ENCL 783
ENCL 784
ENCL 785
ENCL 786
ENCL 787
ENCL 788
ENCL 789
ENCL 790
ENCL 791
ENCL 792
ENCL 793
ENCL 794
ENCL 795
ENCL 796
ENCL 797
ENCL 798
ENCL 799
ENCL 800
ENCL 801
ENCL 802
ENCL 803
ENCL 804
ENCL 805
ENCL 806
ENCL 807
ENCL 808
ENCL 809
ENCL 810
ENCL 811
ENCL 812
ENCL 813
ENCL 814
ENCL 815
ENCL 816
ENCL 817
ENCL 818
ENCL 819
ENCL 820
ENCL 821
ENCL 822
ENCL 823
ENCL 824
ENCL 825
ENCL 826
ENCL 827
ENCL 828
ENCL 829
ENCL 830
ENCL 831
ENCL 832
ENCL 833
ENCL 834
ENCL 835
ENCL 836
ENCL 837
ENCL 838
ENCL 839
ENCL 840
ENCL 841
ENCL 842
ENCL 843
ENCL 844
ENCL 845
ENCL 846
ENCL 847
ENCL 848
ENCL 849
ENCL 850
ENCL 851
ENCL 852
ENCL 853
ENCL 854
ENCL 855
ENCL 856
ENCL 857
ENCL 858
ENCL 859
ENCL 860
ENCL 861
ENCL 862
ENCL 863
ENCL 864
ENCL 865
ENCL 866
ENCL 867
ENCL 868
ENCL 869
ENCL 870
ENCL 871
ENCL 872
ENCL 873
ENCL 874
ENCL 875
ENCL 876
ENCL 877
ENCL 878
ENCL 879
ENCL 880
ENCL 881
ENCL 882
ENCL 883
ENCL 884
ENCL 885
ENCL 886
ENCL 887
ENCL 888
ENCL 889
ENCL 890
ENCL 891
ENCL 892
ENCL 893
ENCL 894
ENCL 895
ENCL 896
ENCL 897
ENCL 898
ENCL 899
ENCL 900
ENCL 901
ENCL 902
ENCL 903
ENCL 904
ENCL 905
ENCL 906
ENCL 907
ENCL 908
ENCL 909
ENCL 910
ENCL 911
ENCL 912
ENCL 913
ENCL 914
ENCL 915
ENCL 916
ENCL 917
ENCL 918
ENCL 919
ENCL 920
ENCL 921
ENCL 922
ENCL 923
ENCL 924
ENCL 925
ENCL 926
ENCL 927
ENCL 928
ENCL 929
ENCL 930
ENCL 931
ENCL 932
ENCL 933
ENCL 934
ENCL 935
ENCL 936
ENCL 937
ENCL 938
ENCL 939
ENCL 940
ENCL 941
ENCL 942
ENCL 943
ENCL 944
ENCL 945
ENCL 946
ENCL 947
ENCL 948
ENCL 949
ENCL 950
ENCL 951
ENCL 952
ENCL 953
ENCL 954
ENCL 955
ENCL 956
ENCL 957
ENCL 958
ENCL 959
ENCL 960
ENCL 961
ENCL 962
ENCL 963
ENCL 964
ENCL 965
ENCL 966
ENCL 967
ENCL 968
ENCL 969
ENCL 970
ENCL 971
ENCL 972
ENCL 973
ENCL 974
ENCL 975
ENCL 976
ENCL 977
ENCL 978
ENCL 979
ENCL 980
ENCL 981
ENCL 982
ENCL 983
ENCL 984
ENCL 985
ENCL 986
ENCL 987
ENCL 988
ENCL 989
ENCL 990
ENCL 991
ENCL 992
ENCL 993
ENCL 994
ENCL 995
ENCL 996
ENCL 997
ENCL 998
ENCL 999
ENCL 1000
LEGEND

Fig 2

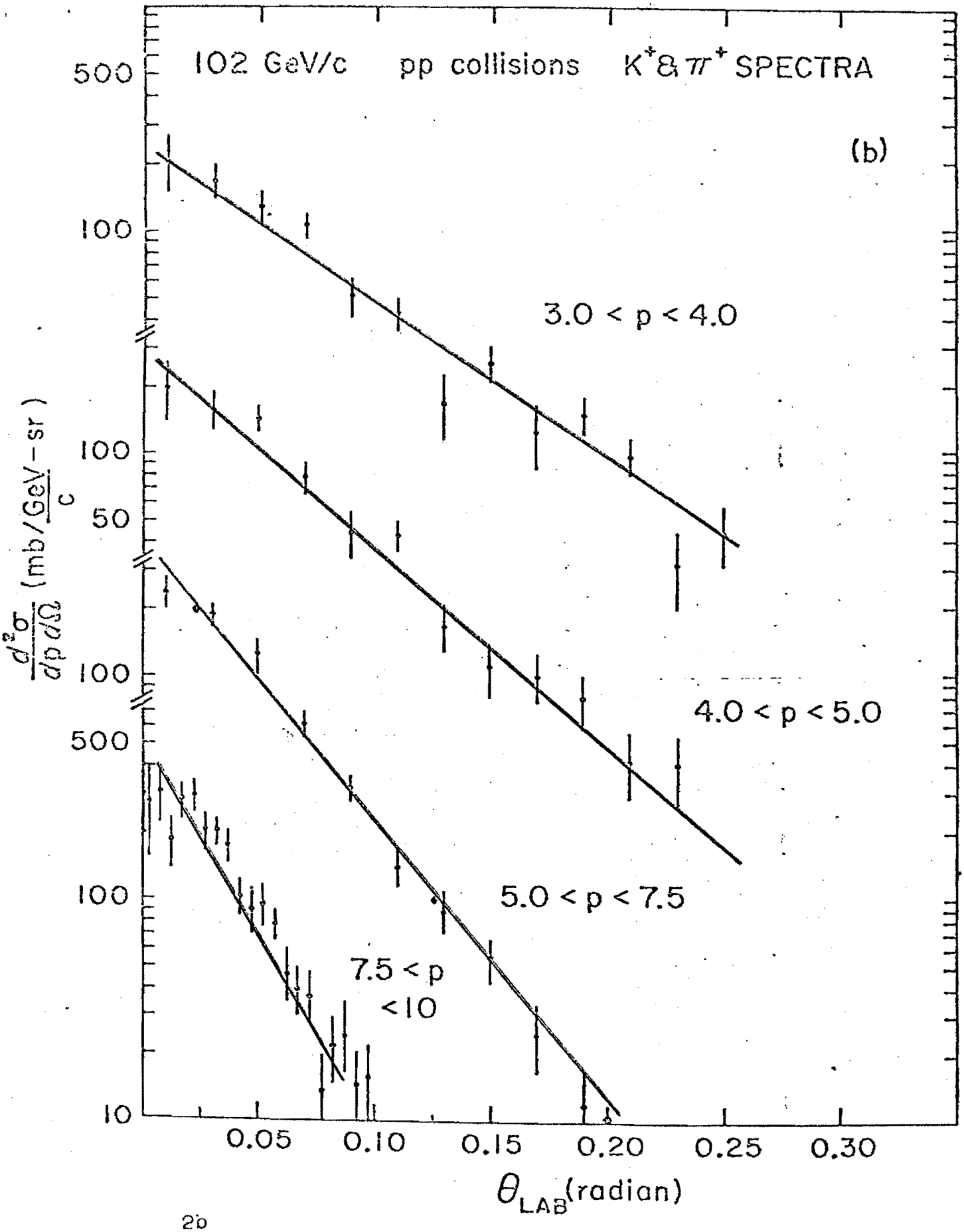
102 GeV/c pp collisions K+& π+ SPECTRA
(b)
3.0 < p < 4.0
4.0 < p < 5.0
5.0 < p < 7.5
7.5 < p < 10
500
100
100
50
100
500
100
10
0.05
0.10
0.15
0.20
0.25
0.30
θLAB (radian)
d²σ/dp dΩ (mb/GeV/c-sr)

Fig. 3

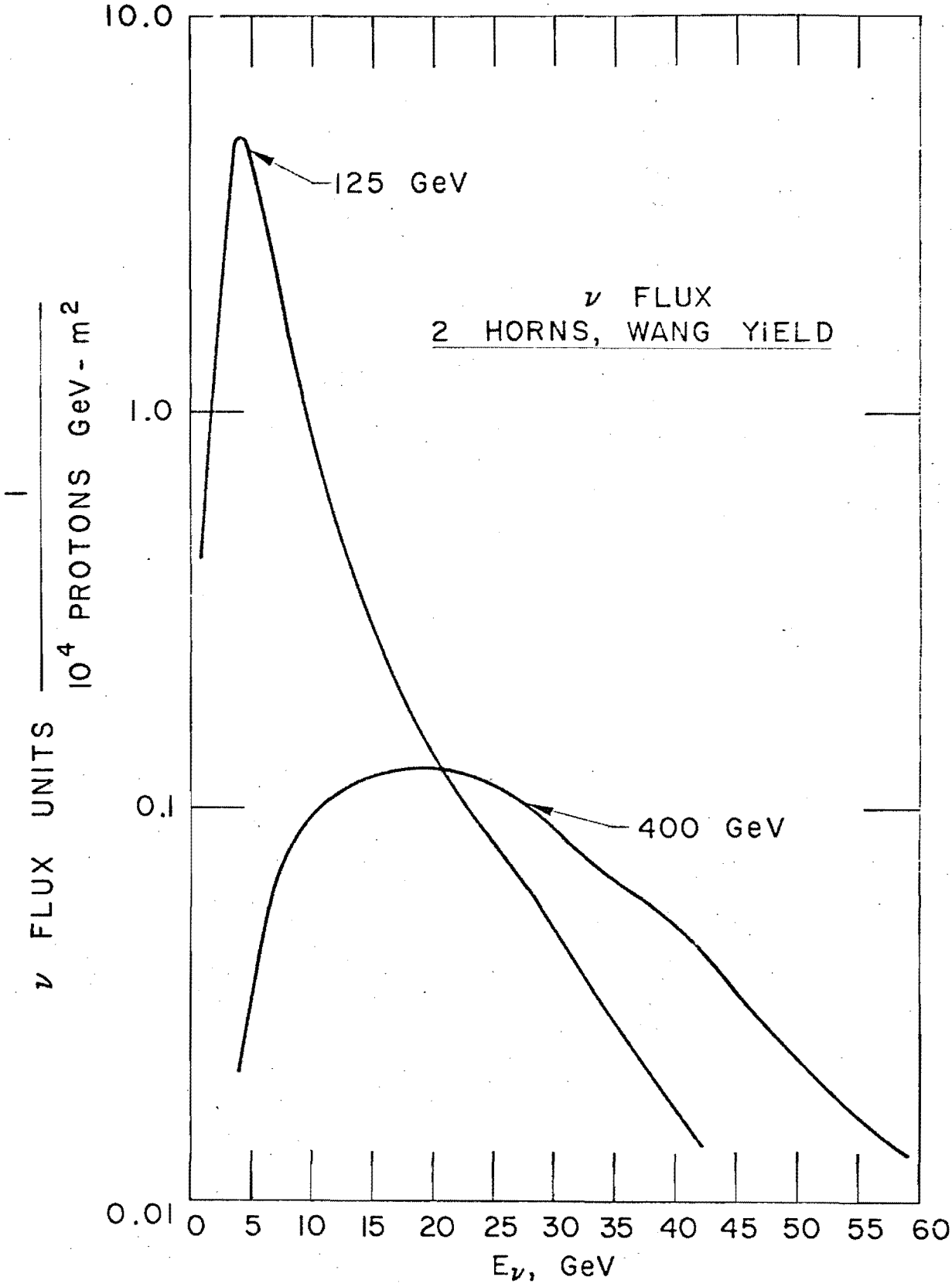
10.0
1.0
0.1
0.01
125 GeV
400 GeV
ν FLUX
2 HORNS, WANG YIELD
ν FLUX UNITS / 10^4 PROTONS GeV - m^2
0 5 10 15 20 25 30 35 40 45 50 55 60
Eν, GeV

Fig. 4

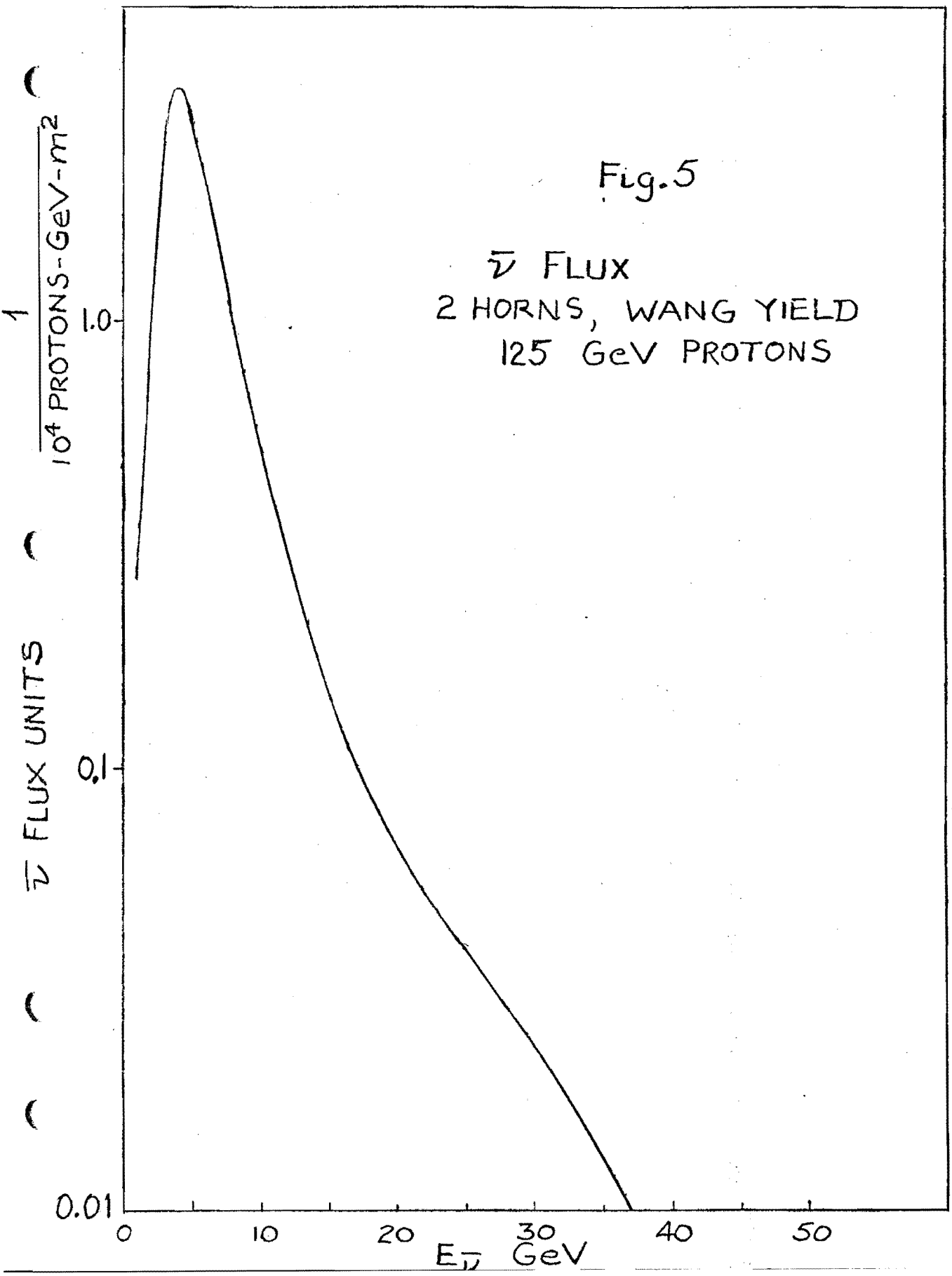
Fig. 5
$\bar{\nu}$ FLUX
2 HORNS, WANG YIELD
125 GeV PROTONS
$\bar{\nu}$ FLUX UNITS
$\frac{1}{10^4 \text{ PROTONS-GeV-m}^2}$
1.0
0.1
0.01
0
10
20
30
40
50
$E_{\bar{\nu}}$ GeV

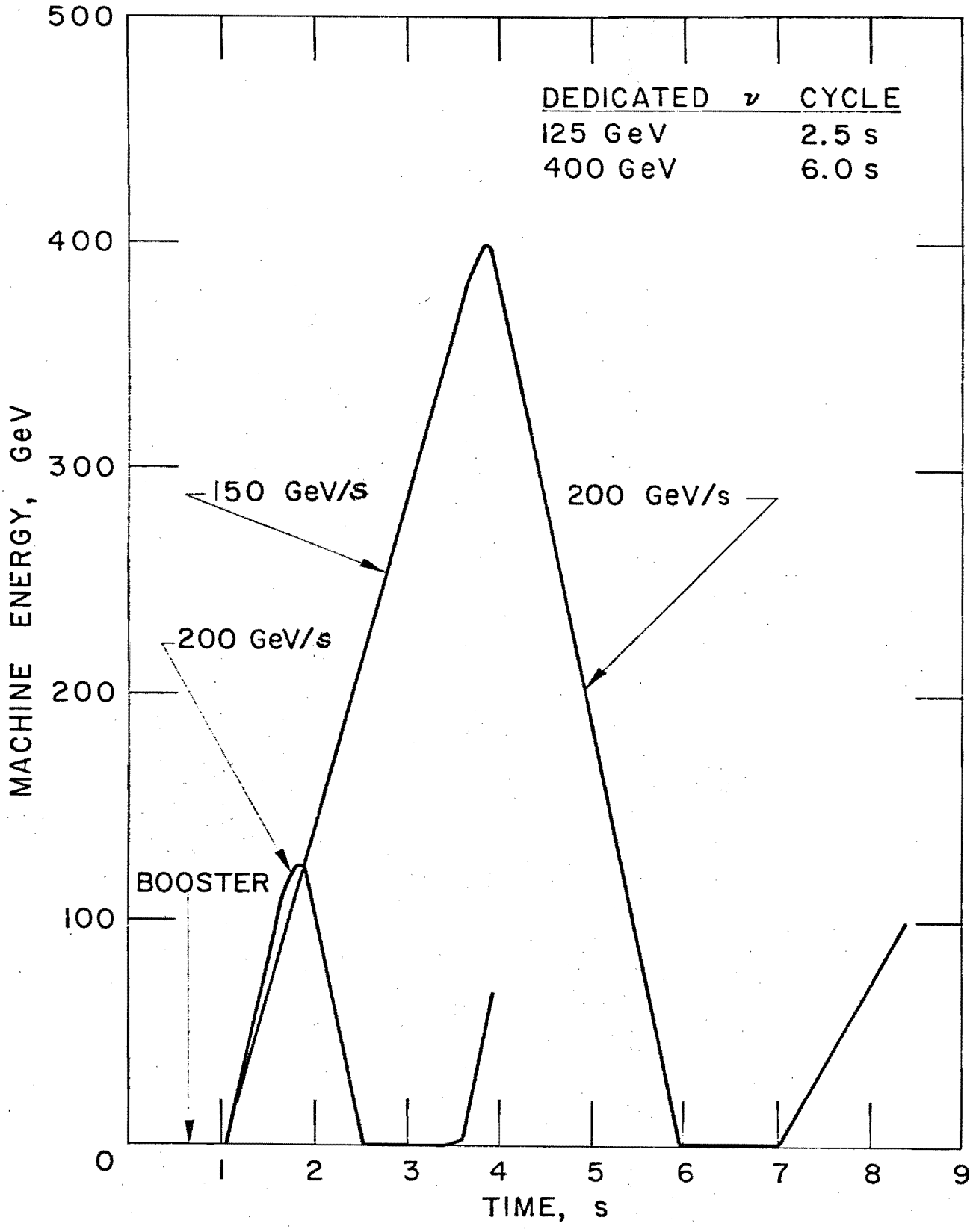
DEDICATED ν CYCLE
125 GeV 2.5 s
400 GeV 6.0 s
150 GeV/s
200 GeV/s
200 GeV/s
BOOSTER
MACHINE ENERGY, GeV
TIME, s
0
100
200
300
400
500
1
2
3
4
5
6
7
8
9

Fig. 6

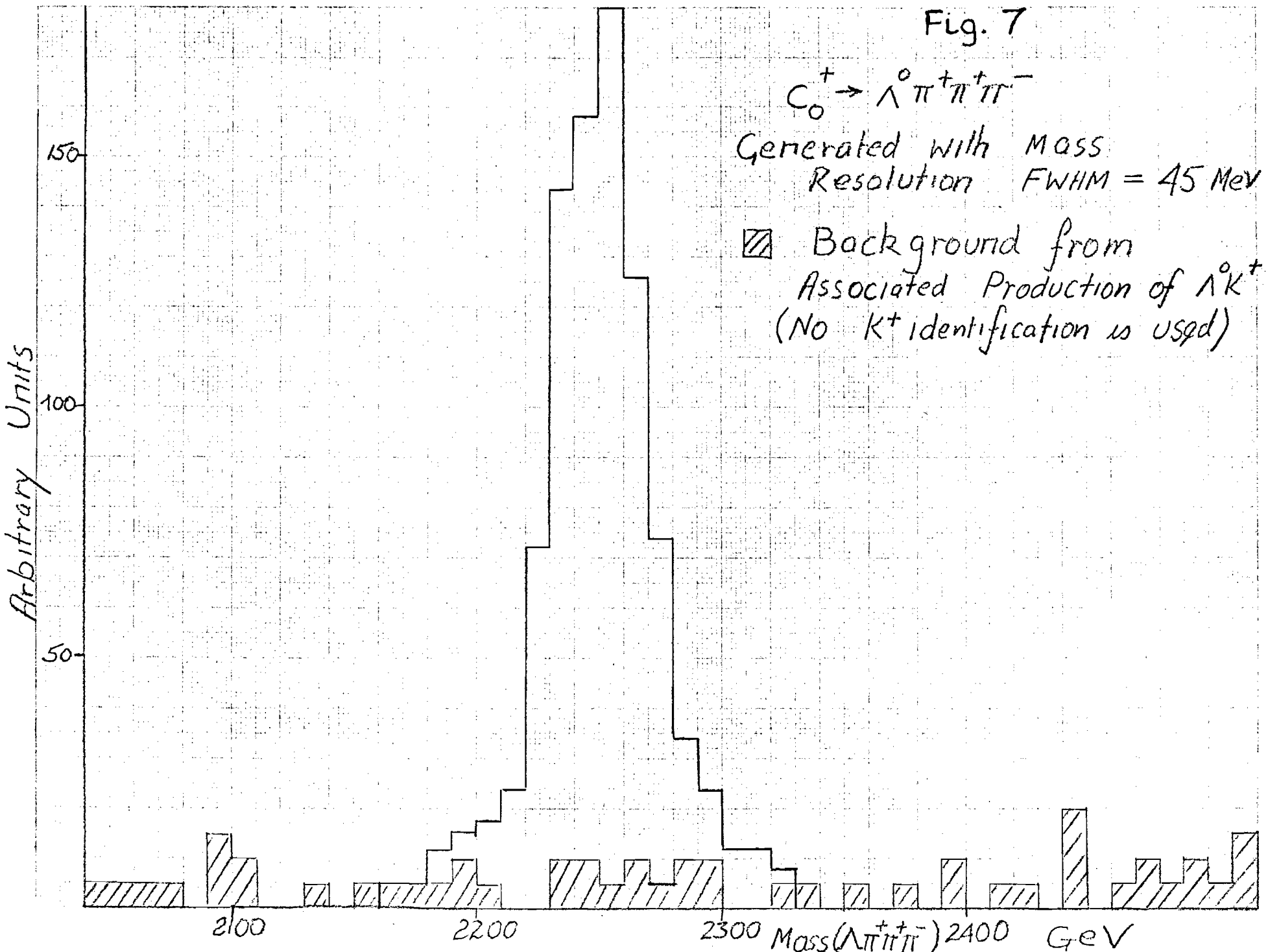
Fig. 7
$C_0^+ \to \Lambda^0 \pi^+ \pi^+ \pi^-$
Generated with Mass Resolution FWHM = 45 MeV
Background from Associated Production of $\Lambda^0 K^+$
(No K^+ identification is used)
Arbitrary Units
150
100
50
2100
2200
2300
Mass($\Lambda\pi^+\pi^+\pi^-$) 2400
GeV

(a)

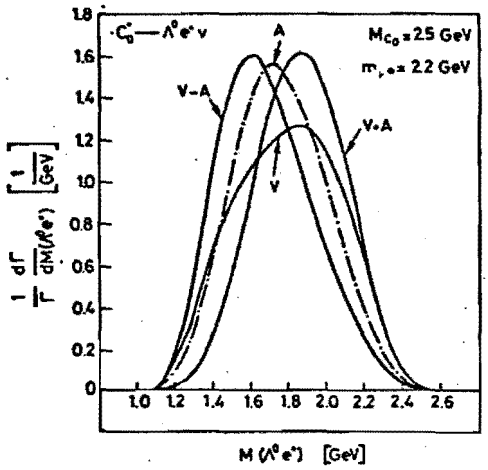

The normalized Mass distribution $\frac{1}{\Gamma}\frac{d\Gamma}{dM(\Lambda e)}$ at $M_{C_0^+} = 2.5$ GeV ; $M_{F^*} = 2.2$ GeV

(b)

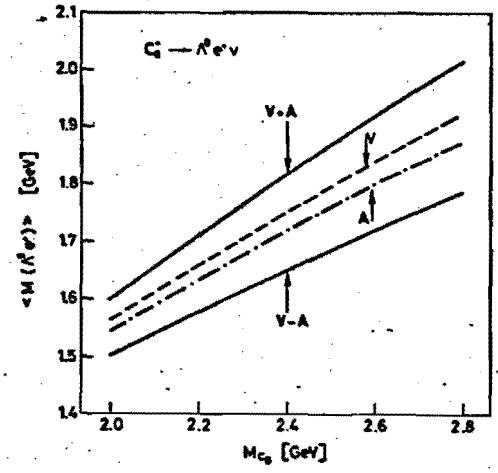

The dependence of $\langle M(\Lambda e)\rangle$ on the Mass $M_{C_0^+}$ for various choices of the Couplings

(c)

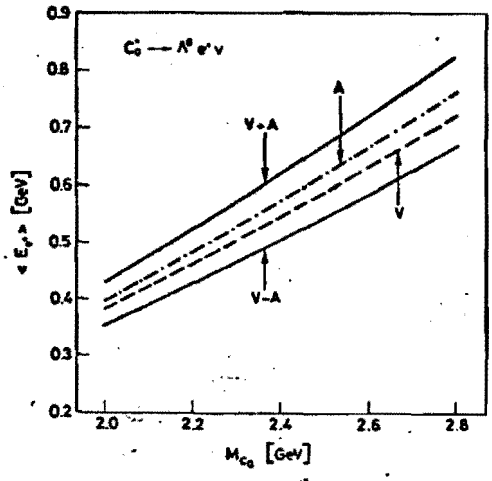

The dependence of $\langle E_{e^+}\rangle$ on the mass $M_{C_0^+}$ for various choices of the couplings

Fig. 8

(a)

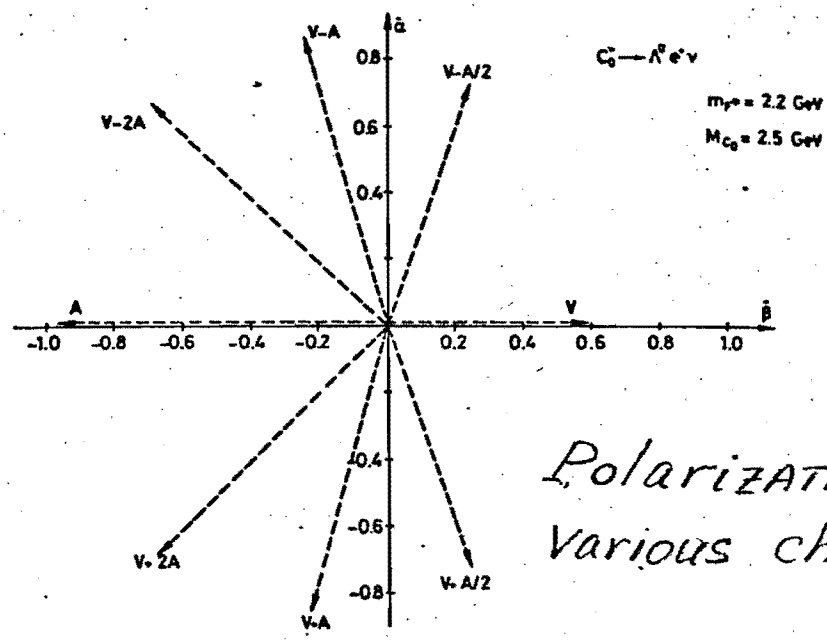

Polarization vector $\hat{\Pi}_{B_f}$ for various choices of the couplings $C_0^+ \to \Lambda^0 e^+ \nu$

(b)

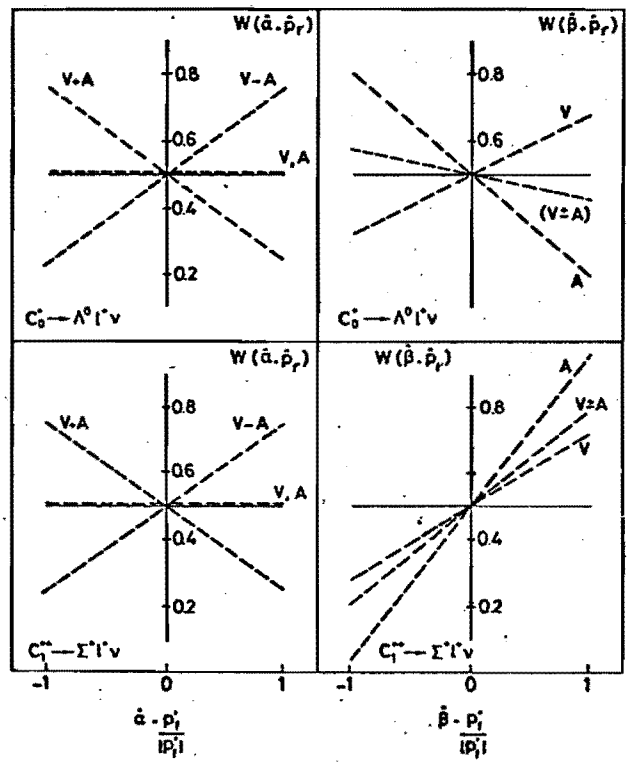

Projected distributions for reaction $C_0^+ \to \Lambda^0 e^+ \nu$ with different couplings

Fig. 9

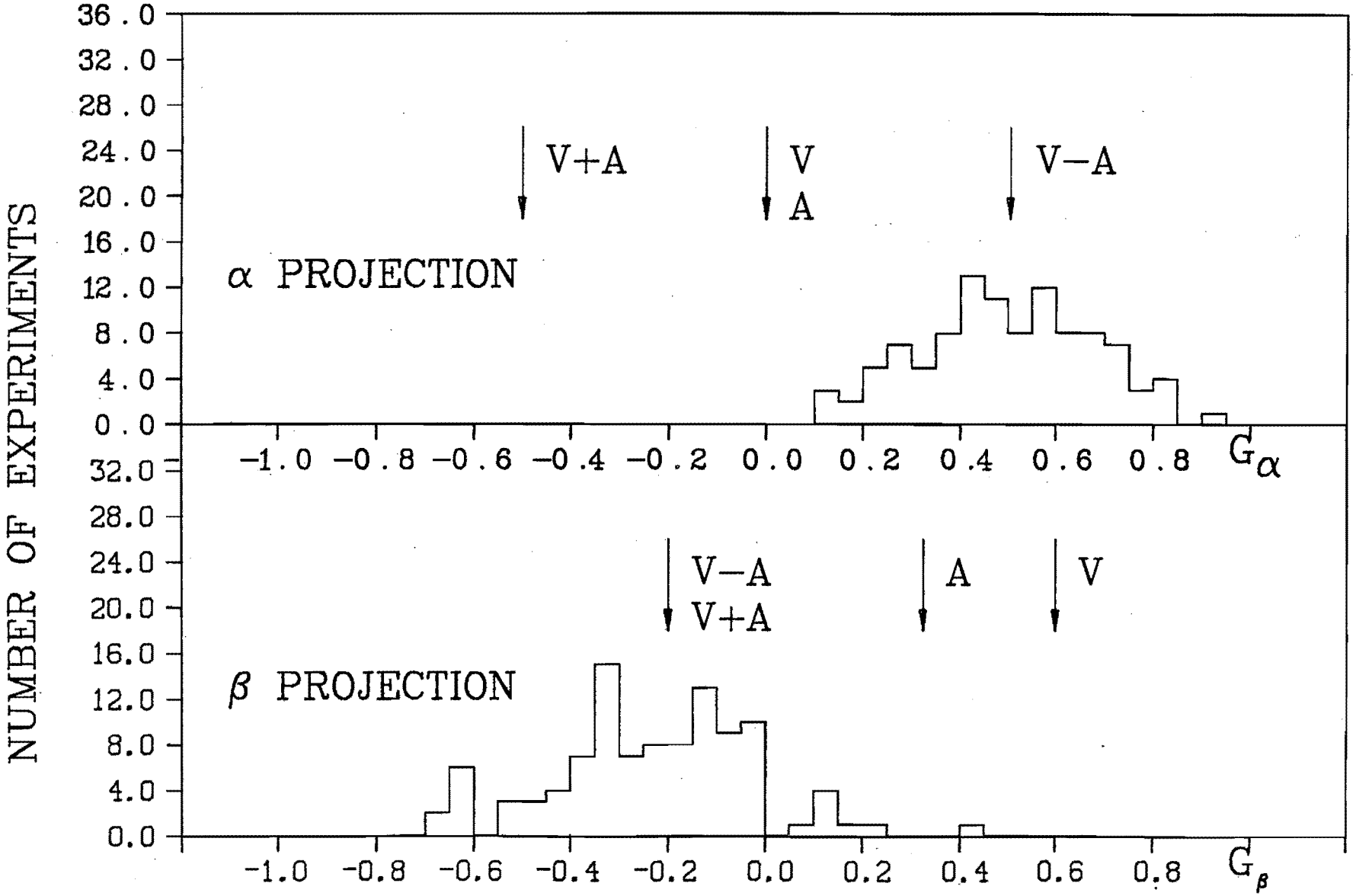
NUMBER OF EXPERIMENTS
36.0
32.0
28.0
24.0
20.0
16.0
12.0
8.0
4.0
0.0
V+A
V
A
V−A
α PROJECTION
−1.0 −0.8 −0.6 −0.4 −0.2 0.0 0.2 0.4 0.6 0.8
G_α
32.0
28.0
24.0
20.0
16.0
12.0
8.0
4.0
0.0
V−A
V+A
A
V
β PROJECTION
−1.0 −0.8 −0.6 −0.4 −0.2 0.0 0.2 0.4 0.6 0.8
G_β

Fig. 10

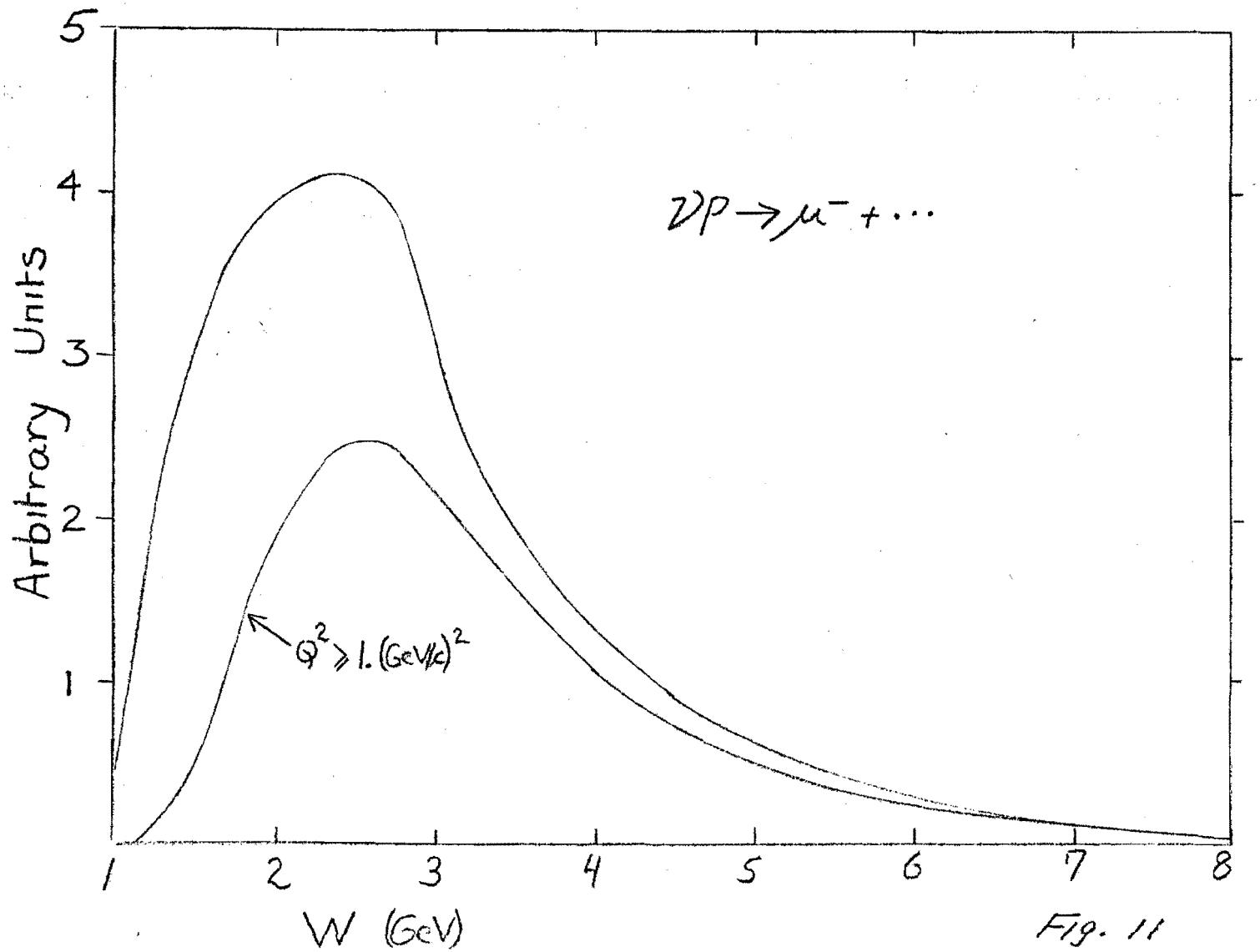
$\nu p \to \mu^- + \cdots$
$Q^2 \geq 1.\,(\mathrm{GeV}/c)^2$
Arbitrary Units
W (GeV)
1
2
3
4
5
6
7
8

Fig. 11

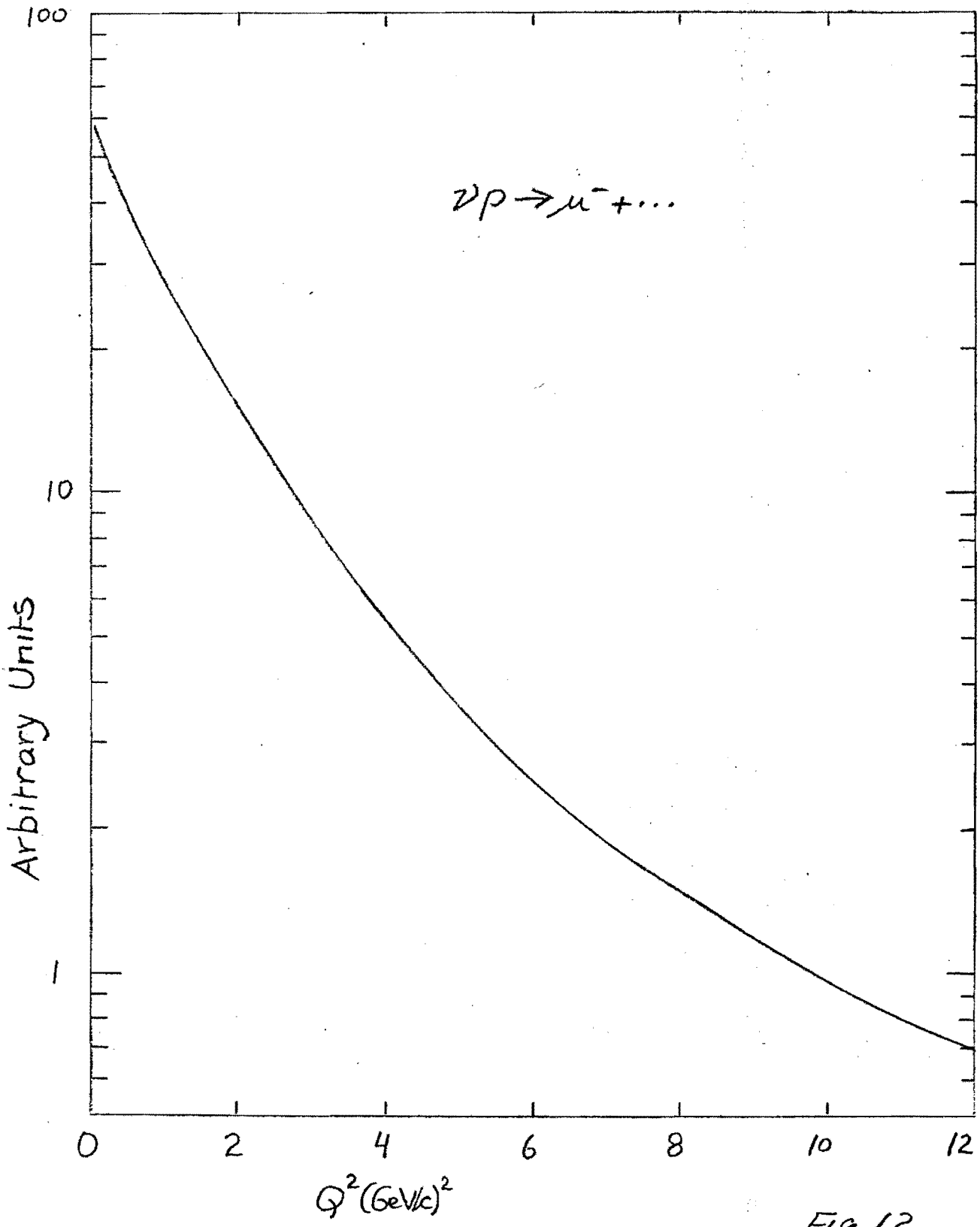

Fig 12

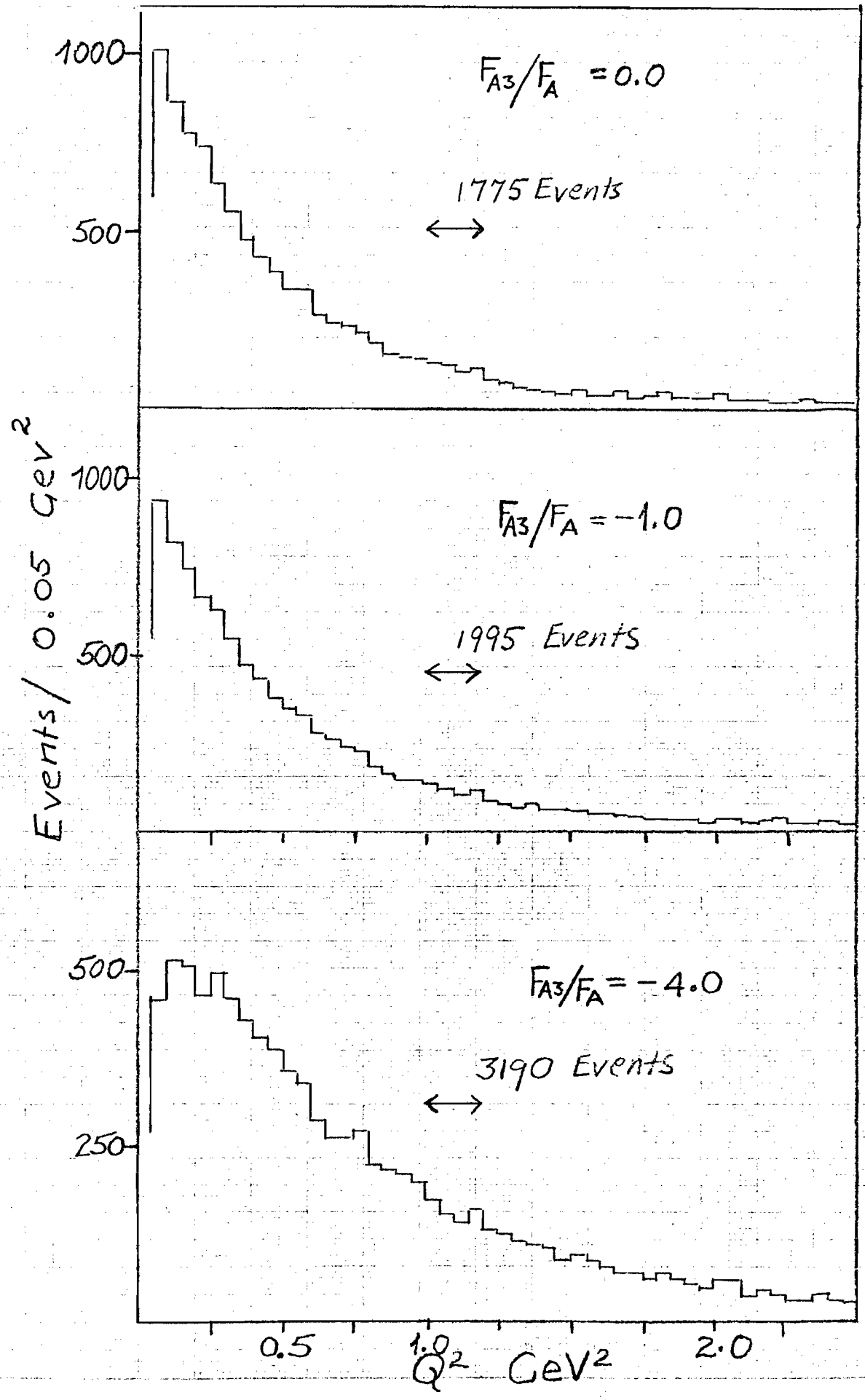
1000
500
$F_{A3}/F_A = 0.0$
1775 Events
1000
500
$F_{A3}/F_A = -1.0$
1995 Events
500
250
$F_{A3}/F_A = -4.0$
3190 Events
Events / 0.05 GeV^2
0.5
1.0
2.0
Q^2 GeV^2

Fig 13

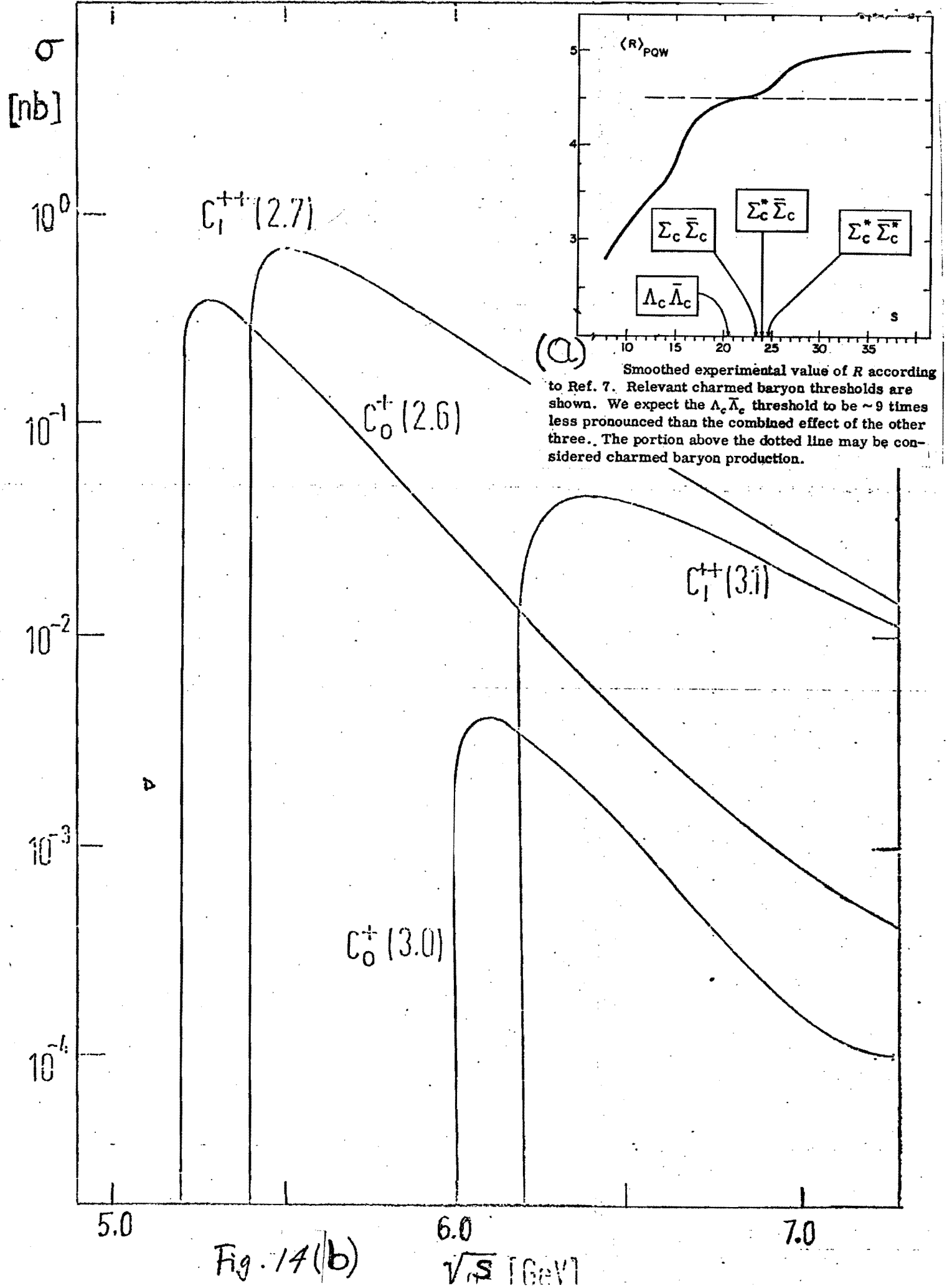

(a) Smoothed experimental value of R according to Ref. 7. Relevant charmed baryon thresholds are shown. We expect the $\Lambda_c \bar{\Lambda}_c$ threshold to be ~9 times less pronounced than the combined effect of the other three. The portion above the dotted line may be considered charmed baryon production.

Fig. 14(b)

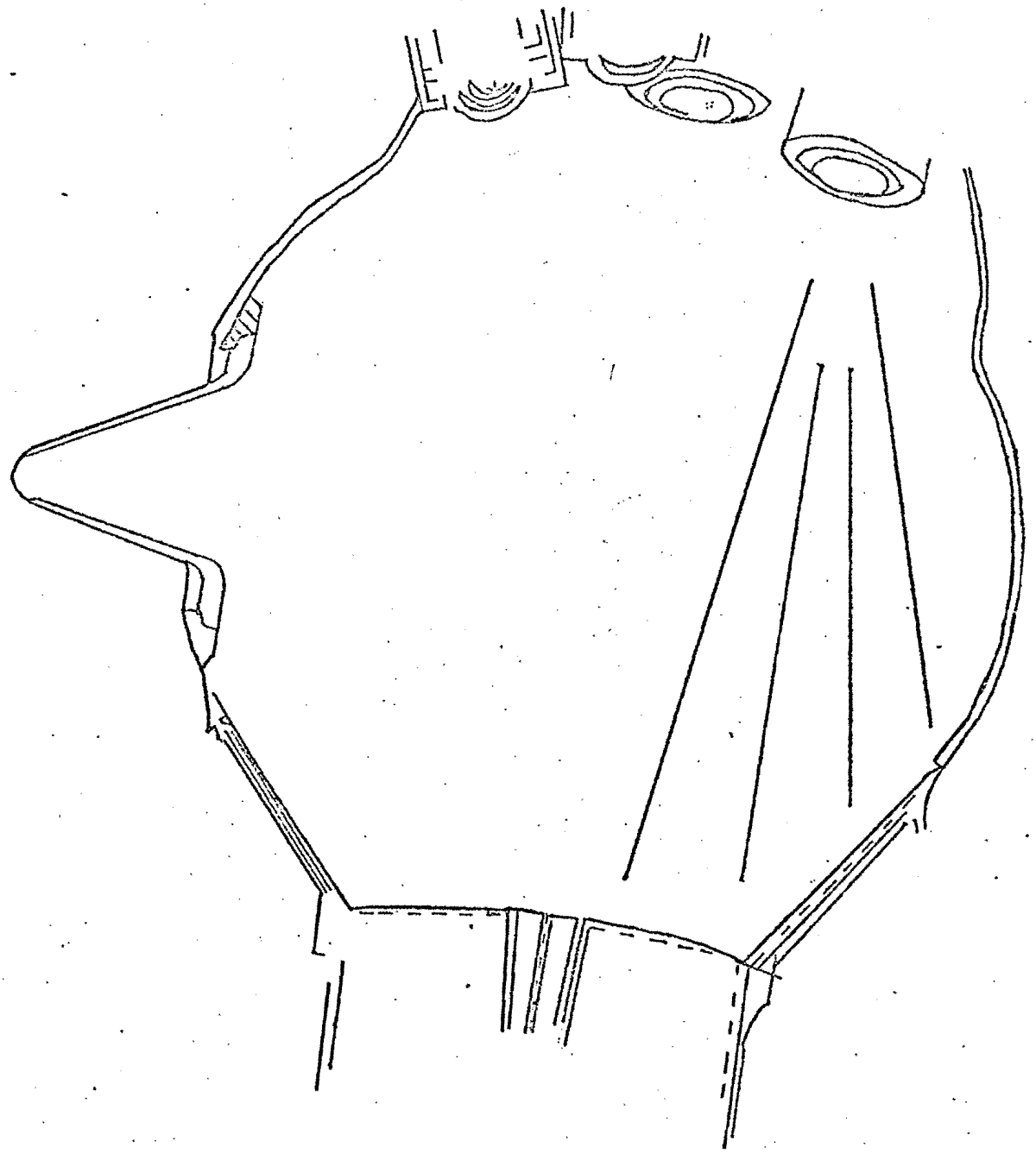

Figure 15